

A.F.M.E.

SEISMIC STUDIES ON THE HDR SITE OF SOULTZ-SOUS-FORETS (ALSACE, FRANCE)

**Alain BEAUCE*, Hubert FABRIOL*, Dominique LE MASNE*,
Claude CAVOIT**, Pierre MECHLER***, Xin Kai CHEN***

* BRGM - SGN/IMRG - BP 6009 - 45060 ORLEANS CEDEX 2 - FRANCE

** CNRS - CRG GARCHY - 58150 POUILLY-SUR-LOIRE - FRANCE

*** Université de PARIS VI - Laboratoire de Géophysique appliquée
Tour 15-25 - 4, place Jussieu - 75230 PARIS CEDEX 05 - FRANCE

**Février 1990
R 30571**

IRG SGN 90

This work has been financially supported
by the European Economic Community (EEC contract n° EN3G-0072-F),
the A.F.M.E. (Agence Française pour la Maîtrise de l'Energie),
and the BRGM (Bureau de Recherches Géologiques et Minières)

**BUREAU DE RECHERCHES GÉOLOGIQUES ET MINIÈRES
SERVICE GÉOLOGIQUE NATIONAL
Institut mixte de recherches géothermiques
B.P. 6009 - 45060 ORLÉANS CEDEX 2 - France - Tél. : 38.64.31.72**

CONTENTS

SUMMARY

1. INTRODUCTION

2. SEISMIC NETWORK

2.1. Seismic probes

2.1.1. Mechanical design

2.1.2. Electronics

2.1.3. Geophones

2.1.4. Cementation

2.2. Data acquisition system

2.3. Network calibration

3. ACTIVE SEISMIC SURVEY

3.1. VSP surveys and reprocessing of the reflection-seismic profiles

3.2. The velocity model

4. RESULTS OF THE SEISMIC SURVEY DURING STIMULATION IN GPK1

4.1. Description of the hydraulic experiment

4.2. General results of microseismicity induced during stimulation

4.3. Location of the events

5. CONCLUSIONS

LIST OF FIGURES AND TABLES

Figure 1	Situation map of the project.
" 2	Three-axis downhole seismic probe.
" 3	Data acquisition system.
" 4	Location map of the surface shots.
" 5	Example of seismograms recorded on the network for a surface shot.
" 6	Results of the orientation of probe 4598, by hodogrammetry on the surface shots.
" 7	Results of the orientation of probe 4616, by hodogrammetry on the surface shots.
" 8	Comparison between walkaway seismic section, VSP and GEOGRAM.
" 9	Migrated seismic sections of lines 84J and 84K.
" 10	Comparison between rough and corrected velocity logs (sonic tool).
" 11	Seismograms recorded on probe 4609 as a function of propagation distance.
" 12	Seismograms recorded on probe 4616 as a function of propagation distance.
" 13	Soultz seismic network geological and velocity models.
" 14	Chronological display of the seismic-event rate, injected volume, and well head pressure.
" 15	Time of occurrence and amplitudes of the seismic events recorded on probe 4616 during stimulation.
" 16	Example of an induced microseismic event.
" 17	Power spectra of some characteristic events.
" 18	Number of seismic events vs. difference in arrival times ($T_s - T_p$) on probe 4616.
" 19	S and P arrival time differences as a function of time and distribution of the maximum amplitudes recorded on probe 4616.
" 20	Example of location processing for event n° 18.
" 21	Microseismic events distribution and interpretations.
" 22	Hypocenters obtained for a ± 1 ms disturbance in the arrival times (event 18).
Table 1	Characteristics of the observation boreholes.
" 2	P- and S- wave velocities evaluated from Sonic logs (corrected by VSP) inside GPK1.
" 3	Spectral analysis of the hydraulically induced events. General trends.

SUMMARY

During the first phase of the French-German Hot Dry Rock geothermal energy project of Soultz/Forêts in Alsace (sponsored by the European Community), a hydraulic stimulation test was undertaken at the bottom ($T = 140^{\circ}\text{C}$) of the 2000-m-deep GPK1 borehole.

The seismic network, installed by BRGM/IMRG to monitor the microseismicity induced in the granite by the stimulation, consists of three-directional probes (especially designed to withstand the rough temperature and corrosion conditions) cemented at the bottom of the three observation boreholes. Once the seismic signals are digitized, automatic detection of the seismic events and storage of the data is performed in real time.

Major faults dipping 60° West affect the thick (1400 m) sedimentary cover and the granitic horst underneath. To get a precise idea of the tectonic context at depth in the immediate surroundings of GPK1 and to complete the existing reflection-seismic profiles, a VSP seismic survey was carried out. For the same purposes, the granite section of the reflection profiles earlier shot by TOTAL, was reprocessed.

During a 3-day stimulation experiment, despite a rather low water flow-rate (3.3 l/s), 58 seismic events were recorded on the network. Results show a general trend of magnitudes decreasing with time, and a spectral content within the frequency range 50-300 Hz for geophones sited 700 to 1200 m away from the stimulated zone.

Seismic activity started 2 hours after the beginning of the stimulation. Two main focal zones were concerned: one close to the stimulated borehole, and the other one deeper than GPK1's bottom. Their activity started simultaneously.

1. INTRODUCTION

Since the early 1970's, two main Hot Dry Rock geothermal energy projects are in progress. The first one, at Fenton Hill(USA), has been carried out by the Los Alamos National Laboratory (Mock J., 1989). Three boreholes were drilled at depths between 3 to 4.5 km and met temperatures ranging from 185°C to 330°C. The second project, at Camborne (UK), has been managed by the Camborne School of Mines (Baria R. et al., 1989 ; Parker R.H., 1989): three boreholes were drilled in the granite to depths of 2100 to 2600 m; maximum bottom temperatures reach 80°C. In both cases, monitoring the induced seismicity was very helpful in defining the stimulated regions, the reservoir growth and the complementary drilling program.

The HDR site of Soultz, in Alsace (northeastern France), was chosen in 1986 on the western side of a very large thermal anomaly which extends over about 4000 km² in the Rhine graben valley. This site overlaps the old Pechelbronn oil-field. This explains the availability of 60 deep wells drilled in the early 1950's and the existence of several seismic-reflection profiles carried out by TOTAL in 1984.

This very favourable situation allowed a good geologic and thermic knowledge of the site, and led to the drilling of a first borehole (GPK1) completed in December 1987. Below a 1400-m-thick sedimentary cover, its final depth was 2000 m in the granite. Temperatures reach 125°C at the bottom of the sedimentary series and 140°C at total depth (Kappelmeyer O., Gérard A., 1989). Thus, compared to the other European HDR projects, a main characteristic of this site is its relatively high temperature at intermediate depth.

To monitor the site during the hydraulic experiments, three old oil wells were successfully recovered in 1987 in the vicinity of the main well GPK1 and instrumented with three-directional permanent probes cemented at their bottom.

A 3-day main hydraulic-stimulation experiment took place in December 1988 at the bottom of GPK1 borehole together with an induced seismicity survey: 58 events were recorded during these 3 days.

The work of the geophysical team of the BRGM/IMRG in this French-German project is described as follows:

- . design, construction, testing, anchoring and orientation of specific seismic probes;
- . data acquisition and processing system;
- . active seismic survey using VSP technique and shots in GPK1;
- . results of the study of the microseismicity induced by stimulation.

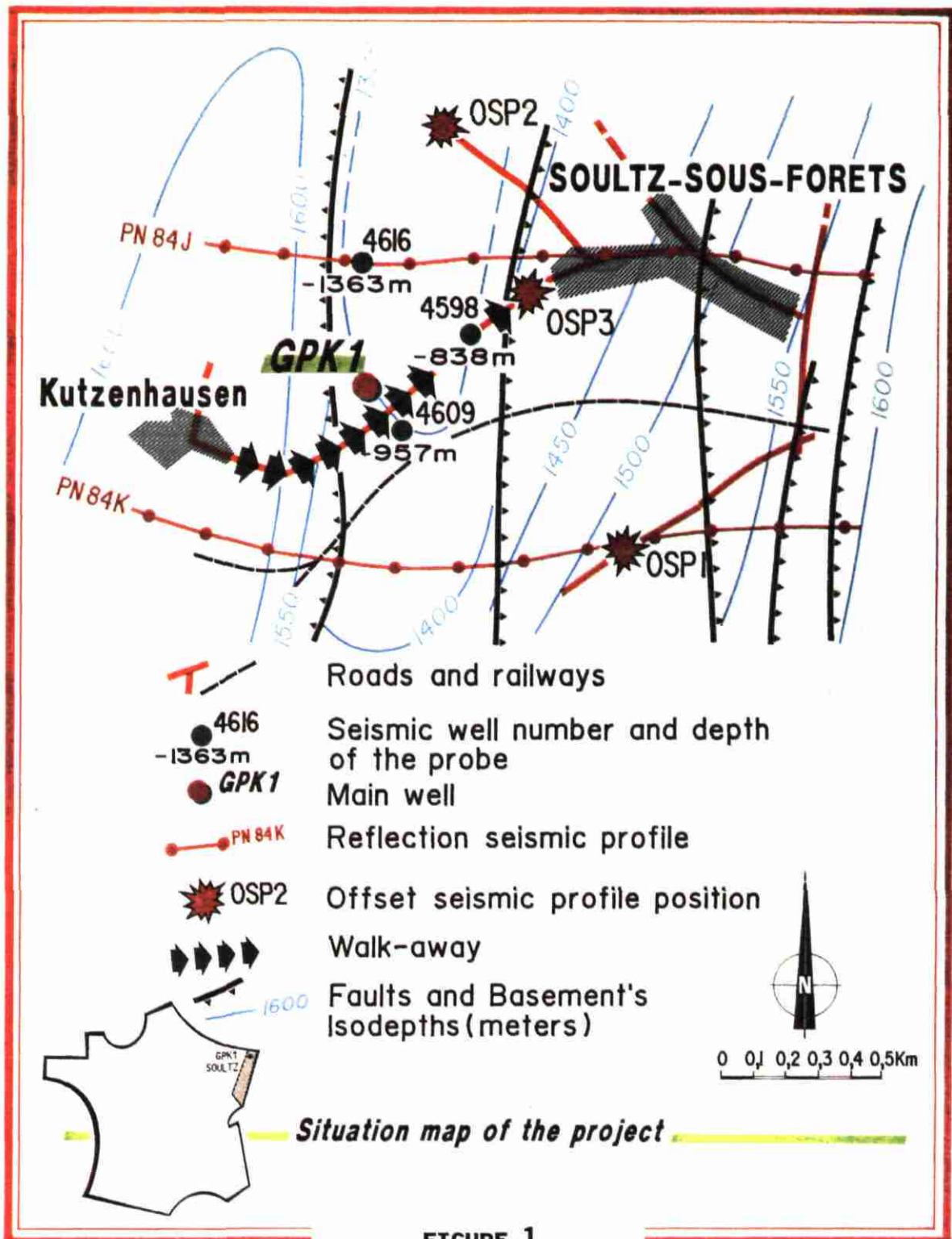


FIGURE 1

2. SEISMIC NETWORK

The three recovered oil-wells, around GPK1, were equipped with seismic probes at total depth (Figure 1). As can be seen on Table 1, the 3D-seismic probes were rather far away from the stimulated zone. Furthermore, only one of them (4616) was located near (20 m above) the granite.

Borehole	Horizontal distances to GPK1 (m)	Bearing with regard to GPK1 (°)	Depth of the probe (m)	Total distance to the stimulated zone (m)	Bottom temperature (°C)
4598	323	N 60	843	1 201	104
4609	100	N 135	963	1 042	114
4616	422	N 355	1 360	767	124

Table 1: Characteristics of the observation boreholes.

2.1 Seismic probes

A prototype 3-axis downhole seismic probe was designed to withstand high temperatures (125°C) and severe corrosion conditions at the bottom of the holes during long periods (several months).

2.1.1 Mechanical design

For the mechanical part of the probe, we modified the original design of the probe developed by IPG Paris for the HDR experiments of Le Mayet de Montagne (Cornet F.H., 1988), keeping the basic concept of the inner column holding the three geophones at right angles from one another (Figure 2).

Due to the high total salinity (100g/l) and temperatures of the surrounding fluids, we used a special stainless steel alloy: Uranus B6. The cylindrical shape of the probe ($\phi=116$ mm, h=500 mm) is suited to the inner diameter of the boreholes (5 5/8") to keep the probe vertical (within a $\pm 5^\circ$ tilt, there is no effect on the correct operation of the geophones).

This probe was linked to the surface by a 3/8" 7-conductor cable (Camesa 7H38RZ) with Tefzel insulated conductors withstanding 220°C for logging tasks and 150°C for permanent completion. Cable-heads were

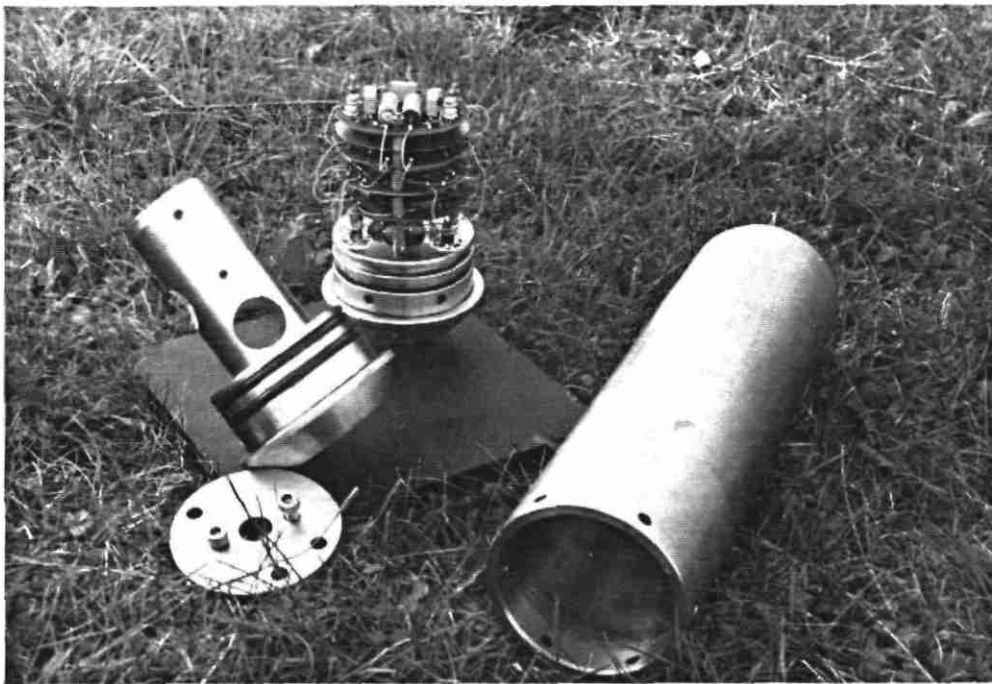


FIGURE 2 - THREE-AXIS DOWNHOLE SEISMIC PROBE

Gearhardt-Owen 1 1/2" 7-conductor High-Temperature ones. Corrosion inhibitors (Norust PA23C & 420M) had been either mixed with the hole water or poured onto the cable and the probes to coat them.

2.1.2 Electronics

The electronic part of the probe (Cavoit C., 1989) had been designed in cooperation with the Centre de Recherches Géophysiques de Garchy (CNRS). Differential analog transmission through two conductors of the cable per geophone (i.e. 6 conductors, out of 7, for the seismic signals) was used to reduce cross-talk between channels to 0.1% at 1000 Hz.

A preamplification of the signals in the probes was necessary because of the long distances between the probes and the surface. The gain (2000) had been fixed from our previous field experiments for oil stimulation (Beauce A., et al., 1988). The electrical feeding of the amplification could be done only through the last remaining conductor and the armour, and thus a DC-DC converter was necessary inside the probe.

High-temperature electronic components were purchased or designed specifically (DC-DC converter) for the experiment and tested by burn-in at 150°C. To minimize heat dissipation at the junctions, the voltage supply of the probe had to be minimal and stable, whatever the intensity of the supplying current; this has been achieved by a voltage source at the well head adapted to the electric consumption of the probe.

After another stage of amplification at the well heads (gain 10), the signals were transmitted to the central recording station (close to GPK1) through 10-conductor cables (SILEC SYT2) buried in the ground, with conductors insulated by pairs. Anti-alias filters (48 dB/oct at 1500 Hz) were applied to the signals just before digitizing.

2.1.3 Geophones

Three Mark-Products High-Temperature L15 geophones (2 horizontal, 1 vertical) with a 20 Hz resonance frequency were inserted into each probe. Despite their narrow standard frequency-range (20-200 Hz), their response curve observed on a shaking table (10 points/decade) appeared flat enough up to 1500 Hz when using shunt-resistances (300 Ω and 600 Ω for horizontal and vertical seismometers respectively) that are different from the standard ones. Their sensitivity at 30 Hz (0.3 and 0.5 V/inch/s respectively) decreases only by 15% at 300 Hz and 35% at 1500 Hz.

The expected frequency band (20-1500 Hz) was broad enough during the field stimulation tests, with the main spectral content of the signals between 50 and 300 Hz.

A 2-week operational test was successfully carried out in June 1988 for two probes in real down-hole conditions before cementation.

2.1.4 Cementation

To avoid resonance, a problem which commonly arises when using clamped tools, it was decided to cement the probes down-hole; this prohibits retrieval of the probes after the experiment, but ensures a good anchoring of the probe against the host rock.

A slow-setting cement (12-14 h) specifically designed by the Institut Francais du Pétrole was poured down the hole by a dump-beller operated by Schlumberger before burying the probe into the liquid cement. Unfortunately, this procedure failed for two of the probes because of the poor hole conditions. In this case, anchoring was achieved by pouring tiny ($\phi = 425$ to 1180μ) zirconium pellets onto the probes from the well head.

2.2 Data-acquisition system

The IMRG numeric data-acquisition system (Figure 3) consists of Hewlett-Packard hardware:

- a fast and powerful (up to 10 channels at 20,000 Hz) Analog/Digital Converter (HP 3852) with a dynamic range of 120 db;
- a HP 9000/350 computer built around a 32-bits MC68020 microprocessor with 8 Megabytes RAM;
- storage units up to 260 Megabytes (2x130 Mbytes disk drives);
- magnetic tape cartridge unit (streamer) for the backup of the data stored on the disk.

The software, adapted from IMRG data-acquisition experiments for the monitoring of an oil-field stimulation, on TOTAL's prospect zones (Beauce & al., 1988), was tested during the orientation blasts and the active seismic program described further on. It allows continuous monitoring of the nine channels of the network and detection of the seismic events recorded at a sampling rate of 8000 Hz per channel.

The detection algorithm used, is based on the ratio of a short-term average absolute value of the signal amplitude over a long-term one. The detection criterion is declared true when this ratio exceeds n times a certain threshold. Channels used for detection during the stimulation were those of the probe 4616. Each time a detection is declared, the system stores 1 second of the 9 channels (300 ms before the detection, 700 ms after) and displays the signal of one channel on the screen.

During the stimulation tests in December 1988, not only the IMRG numeric system was operating, but also a classical analog tape recorder, installed by the Camborne School of Mines team, that recorded continuously during the whole experiment. Sorting out and digitizing of the seismic events recorded on these tapes were then carried out back in the laboratory, which also allowed the recovery of low-magnitude events.

2.3 Network calibration

Precise orientation of the horizontal components of the geophones is helpful in locating the seismic events generated during stimulation. Since there is no orientating device inside our seismic probes, we had

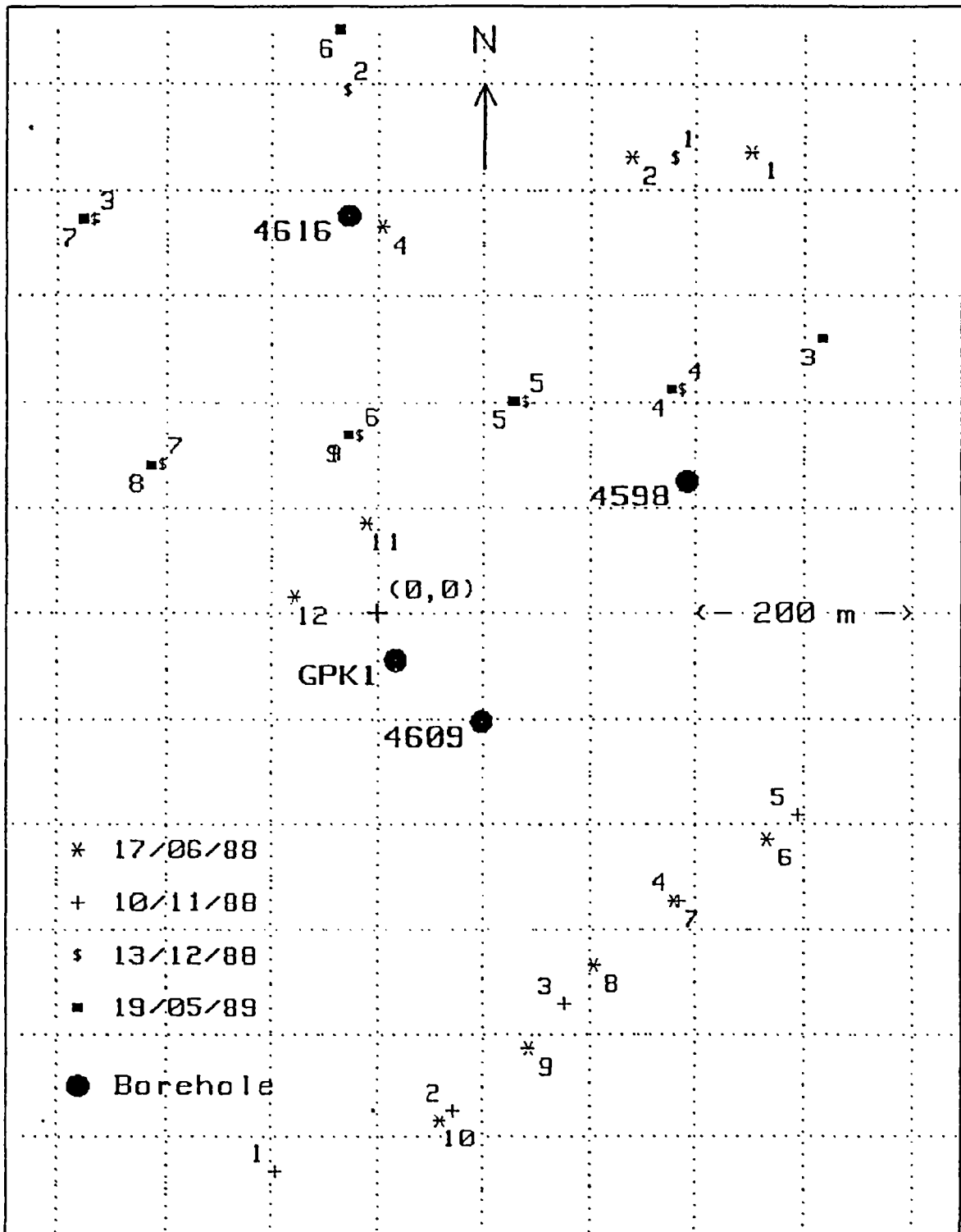


FIGURE 4 - LOCATION MAP OF THE SURFACE SHOTS

no other choice but to use hodogrammetry on the first arrivals of the P-wave transmitted by surface shots. Moreover, this was a way periodically to monitor the proper functioning of the probes and the possible deterioration of the electronic components with time.

Four series of dynamite blasts (1 kg/shot) in very shallow holes (2m) were performed in June, November, December 1988, and again in May 1989 (Figure 4) at horizontal distances from the probes ranging from 100 to 900 m, for various azimuths. Special computer programs were written to record automatically the signals generated by these shots. Figure 5 illustrates the seismograms for a surface shot performed in June 1988. Channel 1, T0, corresponds to a geophone close to the shot. The first arrivals are very clear for every channel, with clear onsets.

The principle of hodogrammetry lies in the velocity hodograms of the P-wave, which have to be linearly polarized along the raypath, and on the assumption of a truly vertical probe (X and Y really horizontal).

If we consider a layered earth, the line described by the velocity hodogram of the X and Y components is the same as the projection of the raypath (source-receiver) onto the horizontal plane passing through the receiver. Rotating this line to make it coincide with the projection of the raypath allows orientation of the X and Y axes of the probe.

This technique has been applied at Soultz despite the complex tectonics of the site (non-tabular model), to get a "statistical" orientation of the probes with several shots (5 to 15) per probe. An illustration of this technique is given in figure 6 with resulting orientations of the Y-axis of the probe in borehole 4598 for 12 shots in June 1988. The mean resulting orientation is N34°, with orientations ranging from N31 to N41°. Poor results from such a technique for probe 4609 at the same time (resulting orientations widely spread) allowed us to identify a defect in the cementation of this probe.

Another type of response for seven shots around borehole 4616 in May 1989, can be seen in figure 7 with two separate groups of resulting orientations of the Y-axis depending upon the azimuth of the shot with regard to the probe:

- N286° ± 3° for shot azimuths between N90° and N180° (shots n° 3, 4, 5),
- N272° ± 1° for shot azimuths ranging from N210° to North, (shots 6, 7, 8).

This series of shots had already been performed in December 1988 with similar results (maximal azimuthal discrepancy of 3° for shots at the same location five months earlier). Hodograms of shots 1 and 9 of figure 7, although not very clear, are shown in this figure because they give a good idea of the repeatability of the response. Unfortunately, shot azimuths between N and N110° have not been covered. This result demonstrates the limits of hodogrammetry with surface shots in such a complex tectonic context: which of the two azimuths is the true one? Obviously, there is an azimuth limit (somewhere between N190° and N210°) on each side of which the waves do not follow the same type of path from the source to the receiver (influence of lateral effects?)

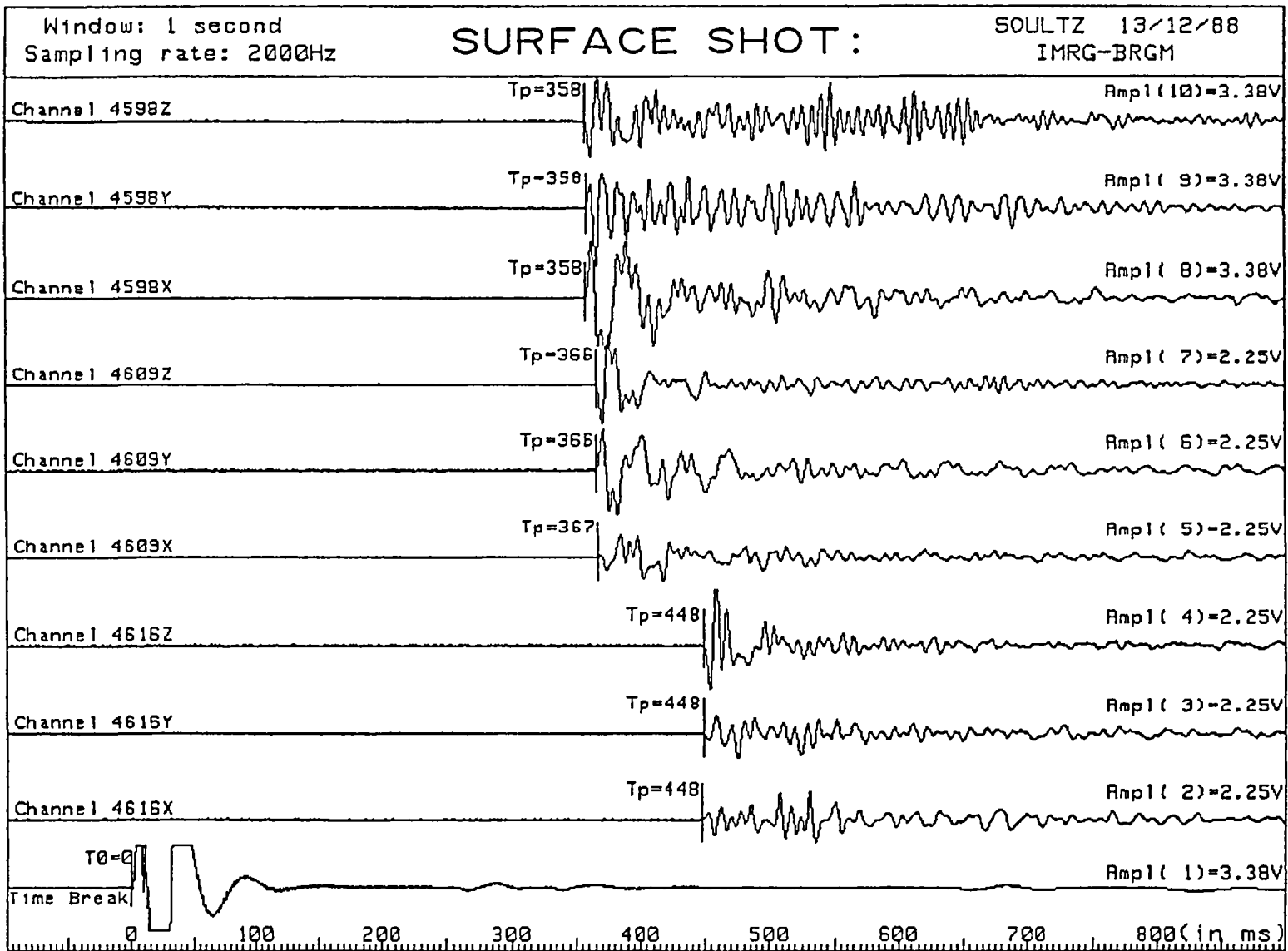


FIGURE 5 - EXAMPLE OF SEISMOGRAMS RECORDED ON THE NETWORK FOR A SURFACE SHOT

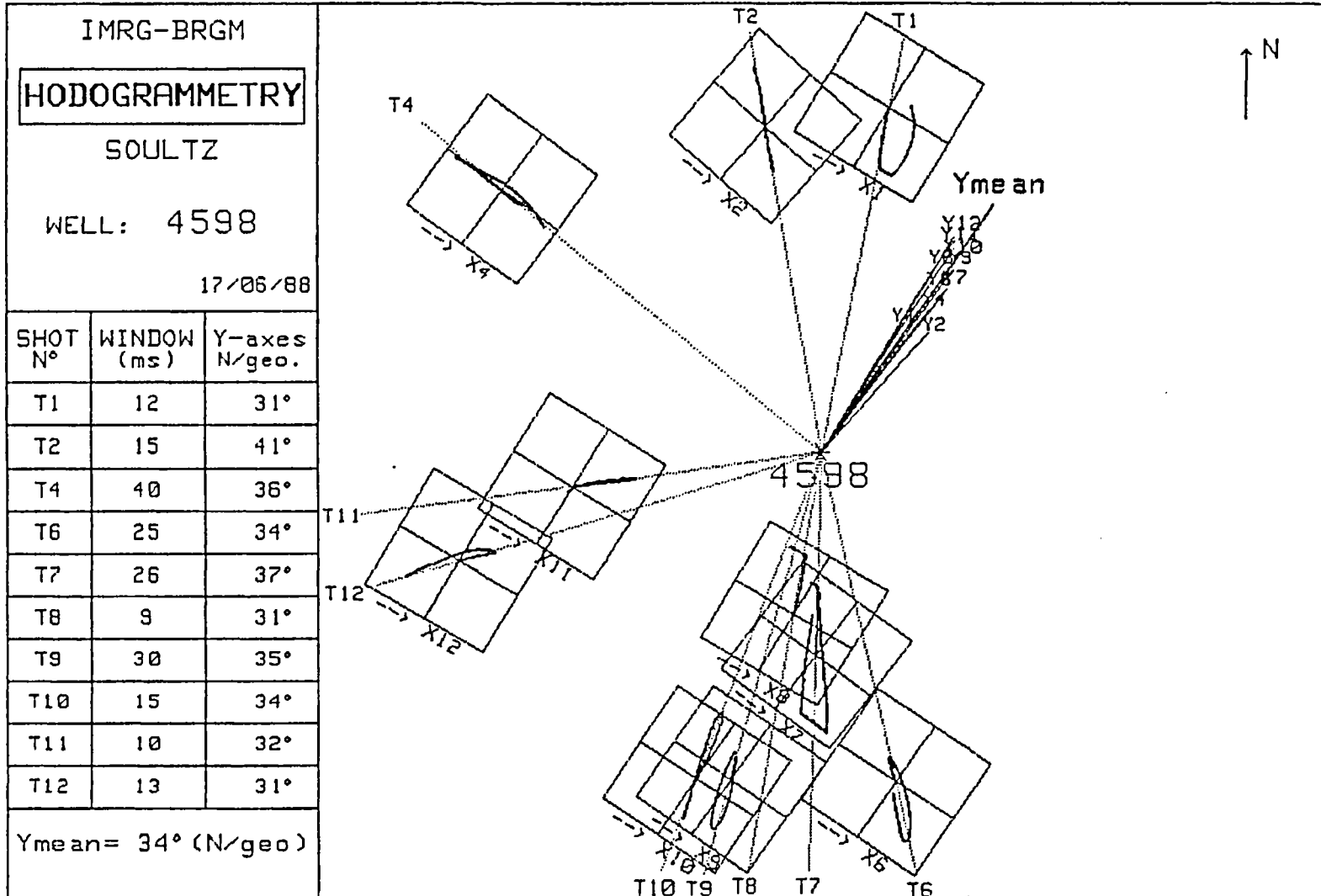


FIGURE 6 - RESULTS OF THE ORIENTATION OF PROBE 4598, BY HODOGRAMMETRY ON THE SURFACE SHOTS

The horizontal offset of the shot does not have a significant effect upon the resulting orientation of the probe, producing only slight differences (2° to 7°) for various offsets at similar azimuths. This is not the case for opposite azimuths, where resulting orientations are quite different (by more than 20° in some cases).

With these surface shots spread in time, we could also test the operation of the probes and obtain information regarding their life expectancy at high temperatures:

- 7 months for probe 4598 (its Y channel failed in January 1989 but the other components were still working in May 1989);

- less than 2 months for probe 4609 (this is likely due to a defect in its cable head down hole) and therefore no orientation of this probe could be obtained;

- more than 9 months for probe 4616, still in proper working order in May 1989 despite the worst temperature conditions (124°C).

In conclusion, hodogrammetry from surface shots produced internally consistent results, but turned out to be inadequate for probe orientation due to the significant non-tabular tectonic features that affect the whole geologic framework. Results would have certainly been improved using down-hole shots with raypaths inside the granite only. We could not directly use this method to locate the events recorded during the stimulation carried out in December 1988, since the probes were too far away from the hypocenters properly to apply hodogrammetry on the signals.

3. ACTIVE SEISMIC SURVEY

The tectonic and geologic context of the Soultz zone can be outlined as a thick sedimentary cover (1400 m at GPK1) on top of a granite horst, with major faults striking NE-SW, dipping 60 to 70° West and affecting the whole series. Geophysical logs run in GPK1 had already shown that possible seismic reflectors could be detected inside the granite, linked to micro-fissured areas (Genter A., 1989).

An active VSP seismic survey was carried out in October 1988 in order to:

- better define the extensions of the fractured zones around GPK1;
- give a velocity model allowing an accurate location of the seismic events to be recorded during the stimulation experiment.

The different field operations carried out by Schlumberger and by IMRG were the following (Figure 1):

- a VSP (Vertical Seismic Profile) along GPK1: 25 receiver levels (spacing 30 m) between 1250 and 1970 m (+ 6 check shots at 100, 300, 500, 700, 900 and 1050 m);
- 3 OSP (Offset VSP) with source offset between 500 and 900 m and 17 receiver levels every 30 m between 1250 m and 1730 m in GPK1;
- a 1-km-long WSP (Walk-Away Seismic Profile) along the NE-SW road joining boreholes GPK1 and 4598, with 26 surface sources every 40 m and 5 receiving levels every 25 m in GPK1 between 1425 and 1525 m depth;
- 21 CST (Core Sample Taker) shots in GPK1 between 1400 and 2000 m;
- 2 shots (200 g Geoflex explosive for each shot) in GPK1 at 1863 m;

During all these operations the downhole seismic probes were operational and the signals recorded and analysed. The source used for VSP surveys was a Vibroseis (3 sweeps per point, transmission bandwidth: 6-90 Hz).

Moreover, the results of the VSP were used to reprocess two reflection-seismic lines, carried out in 1984 by TOTAL, along two E-W profiles (PN 84J and PN 84K) running 0.4 km north and 0.5 km south of GPK1 (see Figure 1). Our aim was to look for specific features in the granite around GPK1, since the main target of the first interpretations was the sedimentary cover.

Shots, using Schlumberger's CST tool as a source, had first been planned before and after the stimulation tests to characterize the system in both situations. Technical problems, such as the erratic behaviour of the CST source at high temperature before stimulation, induced us to abandon this method at that stage.

3.1 VSP surveys and the reprocessing of the reflection seismic profiles.

Figure 8 is a comparison of three kinds of seismic sections (two-way time on all verticals):

- the Walkaway VSP (WSP) obtained after waveshaping deconvolution and NMO (Normal Move-out) corrections using a non-dipping model with velocities consistent with the sonic log measurements;

- the transpose and the corridor stack of the VSP, which are two ways of representing the VSP; the first one gives indications about structures located away from the well axis; the second one is focused on the vicinity of the well and is merely the repetition of the same waveform;

- the GEOGRAM (Trade Mark of SCHLUMBERGER) directly calculated from the density and sonic logs.

In order to seek for fracture zones, we have to consider that they are marked by a decrease in velocity and density, which causes an important reflection of seismic energy with opposite sign. Consequently, we looked for reflectors on the GEOGRAM with reverse polarity, since we knew it was calculated with the compressional velocity and density logs. Effectively, we found 3 events between 1400 and 2000 m depth: at 1590 m (980 ms), 1640 m (1000 ms) and 1825 m (1060 ms). They were well correlated with important altered and fractured zones observed by the analysis of cuttings and by logging methods. They were also present at approximately the same depths on the WSP and VSP sections. The third event (1060 ms) corresponds to the biggest productive water zone (1810 - 1815 m).

Three more events appear on the WSP and the VSP above 2000 m depth at 1530 m (955 ms), 1730 m (1025 ms) and 1910 m (1090 ms). The fact that they do not appear on the GEOGRAM may be explained as follows: they might be due to dipping fractures which do not directly intersect GPK1 and therefore do not affect the acoustic impedance calculated inside the borehole. They cannot a priori be multiples of the downgoing seismic field, since this was removed by the deconvolution.

On the other hand, two other important reflectors are observed on both the VSP and WSP: one just beneath GPK1's bottom (1120 ms) and the other at 1145 ms (\approx 2100 m), SW of GPK1. At present we have no direct information about them, but we can suppose that they are also altered and fractured zones.

Two other major structures appear on the WSP:

- a discrepancy in the reflections for horizontal offsets varying from + 50 m to 130 m NE of GPK1, which can also be noticed on the OSP1 and OSP3 seismic sections. This could be due to a fault dipping 60 to 70° NE located some tens of meters east of GPK1 and visible in the granite between 1000 and 1200 ms (1650 and 2200 m depth - fault F1);

- an interruption in the reflections for offsets varying from + 60 m to 0 m between 1070 and 1180 ms (1850 and 2150 m depth), which

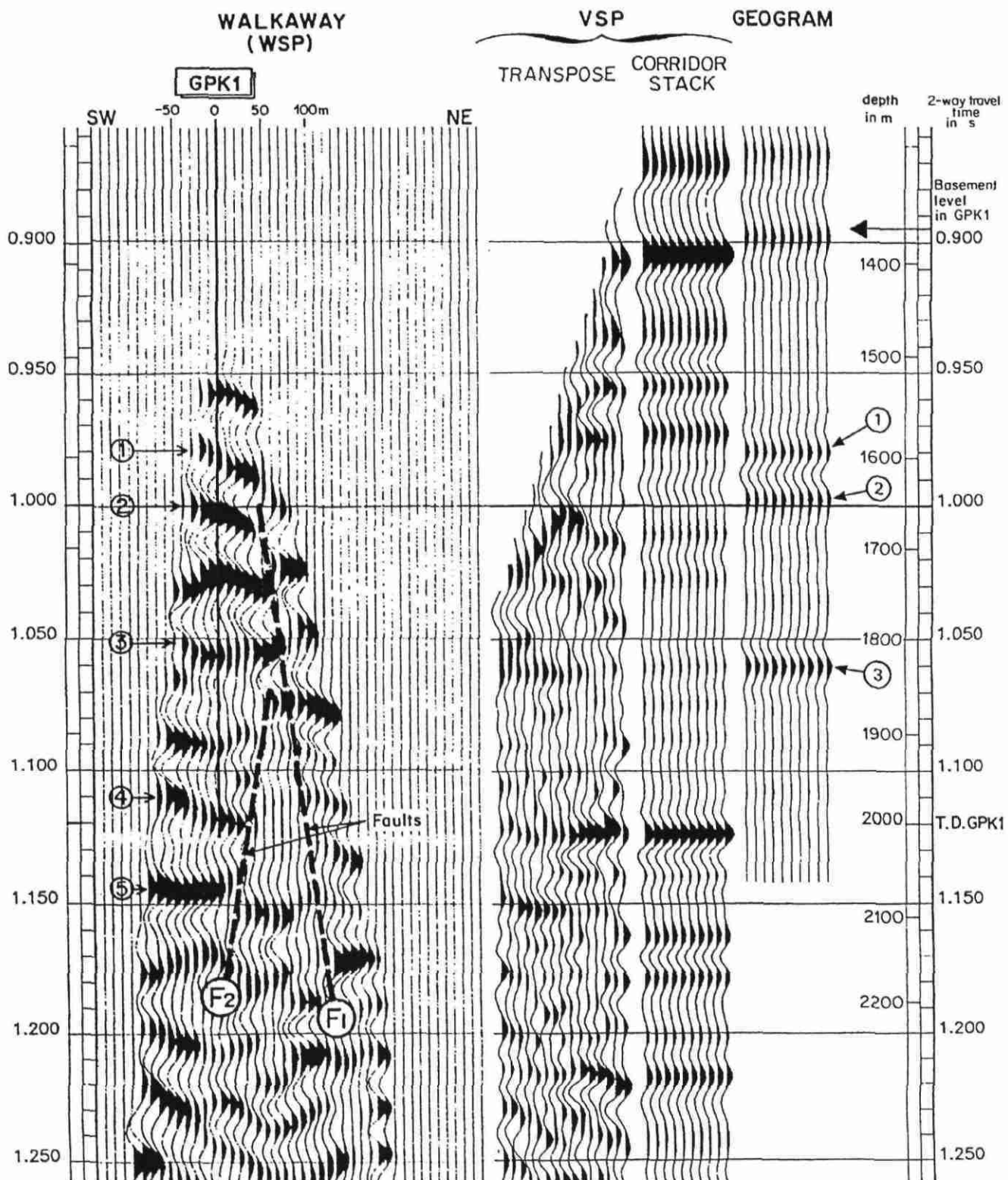


FIGURE 8 - COMPARISON BETWEEN WALKAWAY SEISMIC SECTION, VSP AND GEOGRAM

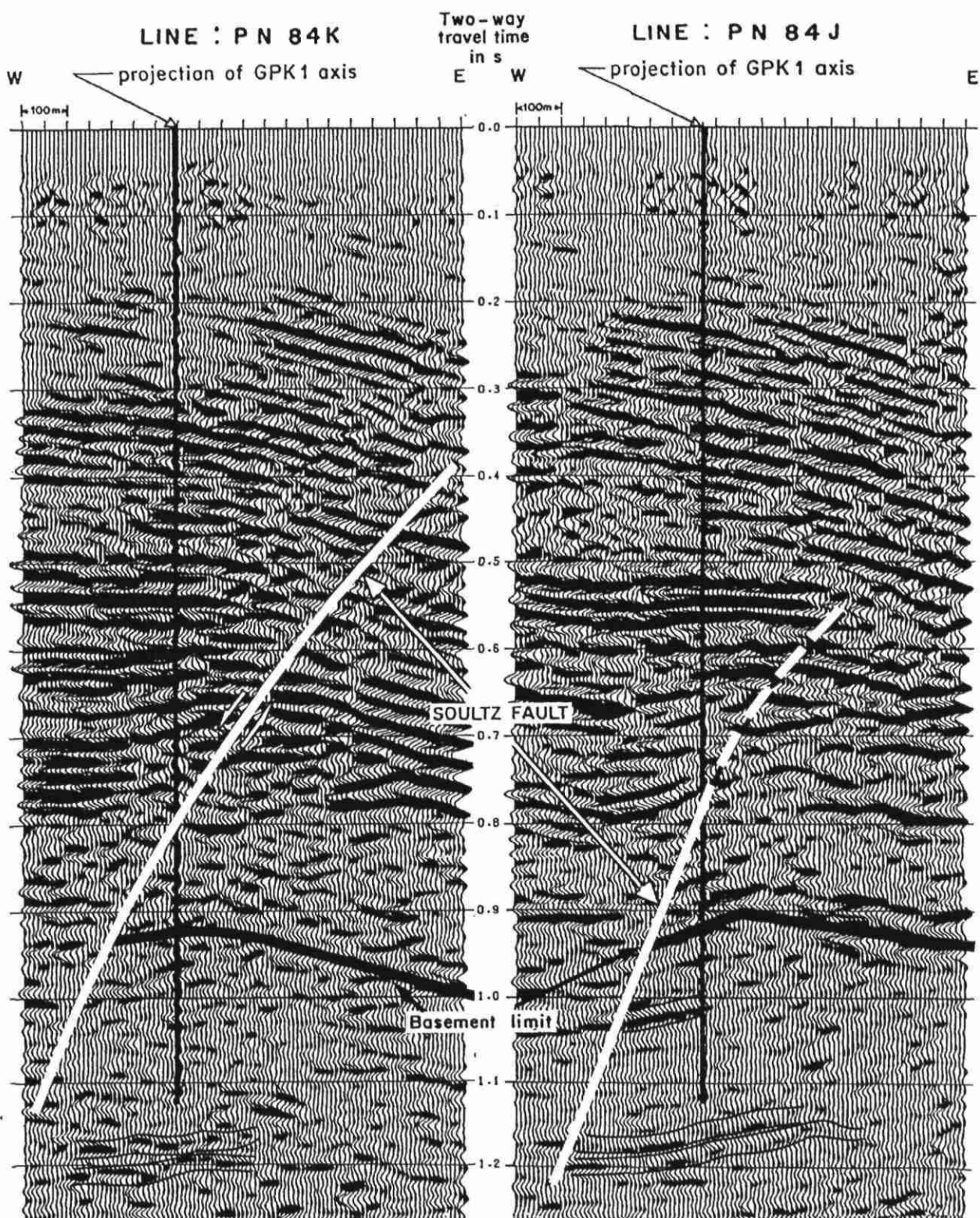


FIGURE 9 - MIGRATED SEISMIC SECTIONS OF LINES 84J AND 84K

could correspond to another fault dipping SW and crossing the axis of GPK1 150 m beneath its bottom (fault F2).

The reprocessing of the TOTAL seismic-reflexion profiles was undertaken as an attempt to correlate the structures observed along and around GPK1 with the corresponding granite area north and south of it.

Figure 9 shows a part of the migrated sections of line 84 J and 84 K, using a velocity model deduced from a structural interpretation of the whole area (Cautru J.P., 1989) and the active seismic survey in GPK1. For convenience both figures are limited to the vicinity of the projection of GPK1 onto the lines.

On line 84 K, sited 500 m south of GPK1, the basement begins at about 920 ms and two well-defined reflectors intersect the projection of the GPK1 axis at 1175 and 1200 ms. Taking into account that the basement in GPK1 is met at 900 ms, it is possible to correlate these reflectors with the events found on the VSP and the WSP at 1140 and 1170 ms respectively.

On line 84 J, sited 400 m north of GPK1, the basement is met at 925 ms, that is a 25 ms difference with GPK1's case. Three reflectors appear between 950 ms and 1200 ms. The first one, at 1020 ms, could correspond to the thick fractured zone at 1590-1640 m in GPK1. The two other ones, sited at 1160 and 1180 ms, correspond roughly to the reflectors noted on the VSP and the WSP at 1140 and 1170 ms. Given the relatively long distances between both sections and GPK1 we do not have enough elements to follow these fractured (or altered) zones from point to point. We merely note their possible existence on the reprocessed sections. This kind of information could be useful in the further stage of the project.

Coherency filters were applied to the migrated sections in order to find the better dip of the oblique reflectors. Good coherencies were found for dips of 35-45° west, which agrees with the main trend of the western flank of the Soultz horst.

No other striking feature appears clearly in the granite part of the sections; the reason could be that this survey was focused on the study of the sedimentary cover. Nevertheless, major features were discovered or pointed out by the active seismic survey, and we shall see afterwards their possible connections to the stimulated zones. Furthermore, the active seismic methods (including cross-hole survey whose results could not be exploited) are the only presently available that give a 3-D image of the well surroundings.

3.2 The velocity model

In order to locate the events induced by stimulation, a tabular three-layer velocity model was built on the basis of the results obtained by the active seismic program mentioned above. Two methods were used to estimate such velocities:

- interval velocities given by sonic logs operated by Schlumberger in GPK1 at the end of the drilling;

- transit times for shots fired inside GPK1 at different levels and recorded on the IMRG downhole network.

Figure 10 illustrates the comparison between P- and S- wave velocities evaluated from the sonic log (not corrected) and the adjusted interval velocity of the P wave, given by the same sonic log corrected after drift calculation between sonic time and seismic time, owing to VSP.

Depth	Layer	Vp (m/s) (Sonic+VSP)	Vs (m/s) (Vp/1.735)
860 m	Muschelkalk	3620	2070
900 m	Buntsandstein	4410	2520
1376 m	Granite	5640	3250

Table 2: P- and S- wave velocities, evaluated from Sonic logs (corrected by VSP) inside GPK1.

The left column of Table 2 gives the values of P-wave velocities evaluated by this method for each layer of the model, using the interval velocities averaged over the layer thickness. S-wave velocities were calculated with the P interval velocities and the mean Vp/Vs ratio obtained with sonic logs (i.e. 1.735).

To complete these results, CST (Core Sample Taker) shots were carried out at different depths in GPK1 inside the granite. But, due to problems with the CST and to the poor quality of the signals (Figure 11) recorded by the probes located above the granite (explosive charge too weak), the only available results for probes 4598 and 4609 were obtained through stacking of the waveforms corresponding to shots inside the uppermost levels (between 1400 and 1500 m).

For the probe in hole 4616, P- and S-wave onsets were clear enough to allow correct calculation of P and S velocities, between 1400 and 2000 m, every 40 m. Figure 12 is a reduced propagation-distance versus time display of the different waveforms recorded on probe 4616 (X component), during the CST experiment. Accurate estimations of P- and S-wave velocities could thus be obtained (Vp= 5680 m/s and Vs=3370 m/s). The same values were observed for two 200 g shots fired at 1863 m inside GPK1. P-wave velocities obtained by the two approaches, gave results that are quite comparable (less than 1% difference). Nevertheless, dramatic differences for the Vp/Vs ratio were observed: 1.689 for the shots versus 1.735 for the sonic logs between 1400 and 2000 m. This difference was probably due to the limited radius of investigation of

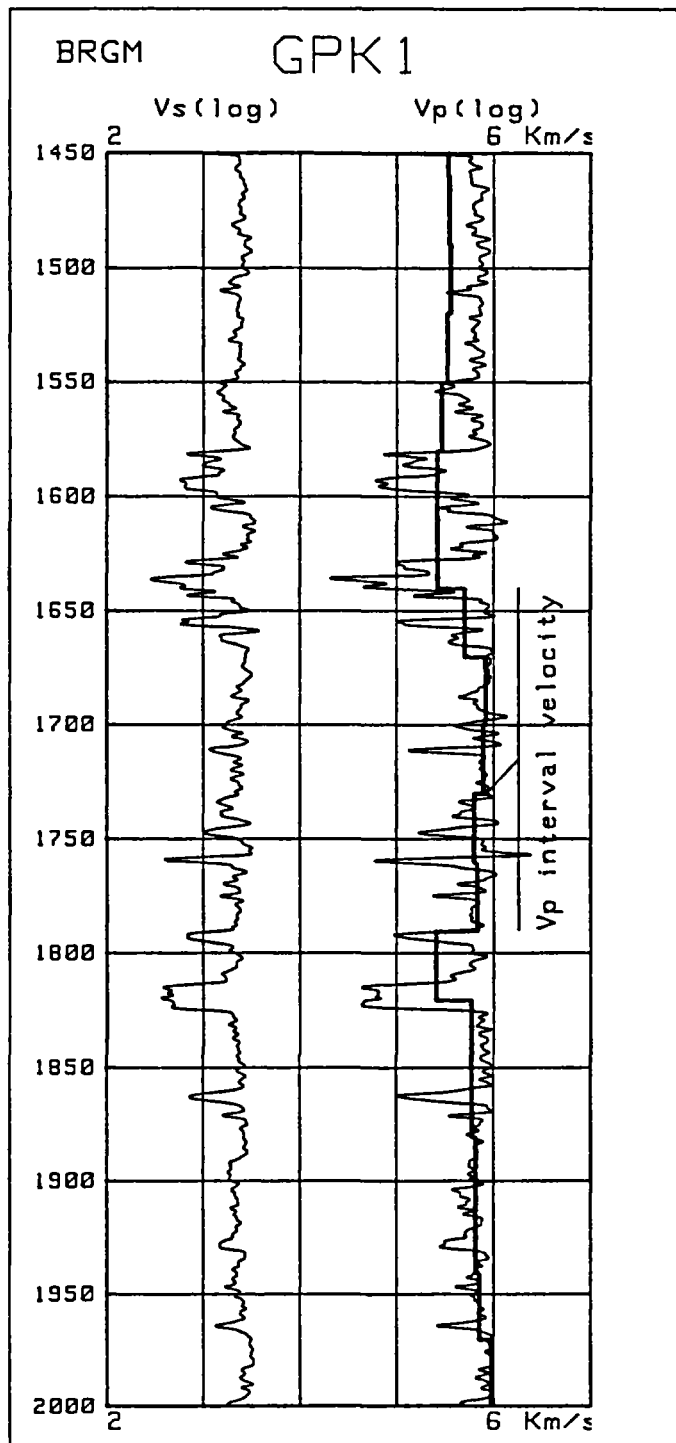


FIGURE 10 - COMPARISON BETWEEN ROUGH AND CORRECTED VELOCITY LOGS
(SONIC TOOL)

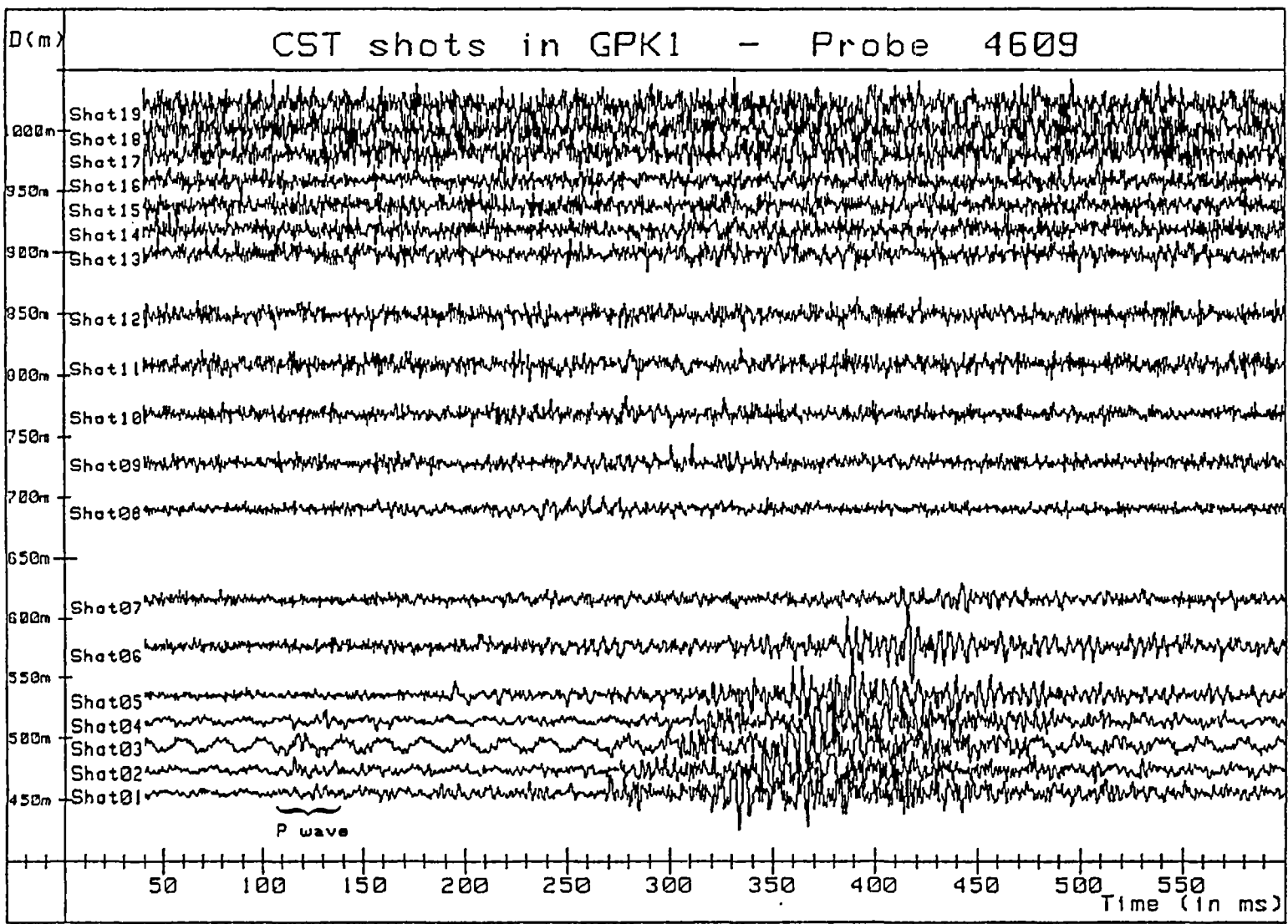


FIGURE 11 - SEISMOGRAMS RECORDED ON PROBE 4609 AS A FUNCTION OF PROPAGATION DISTANCE

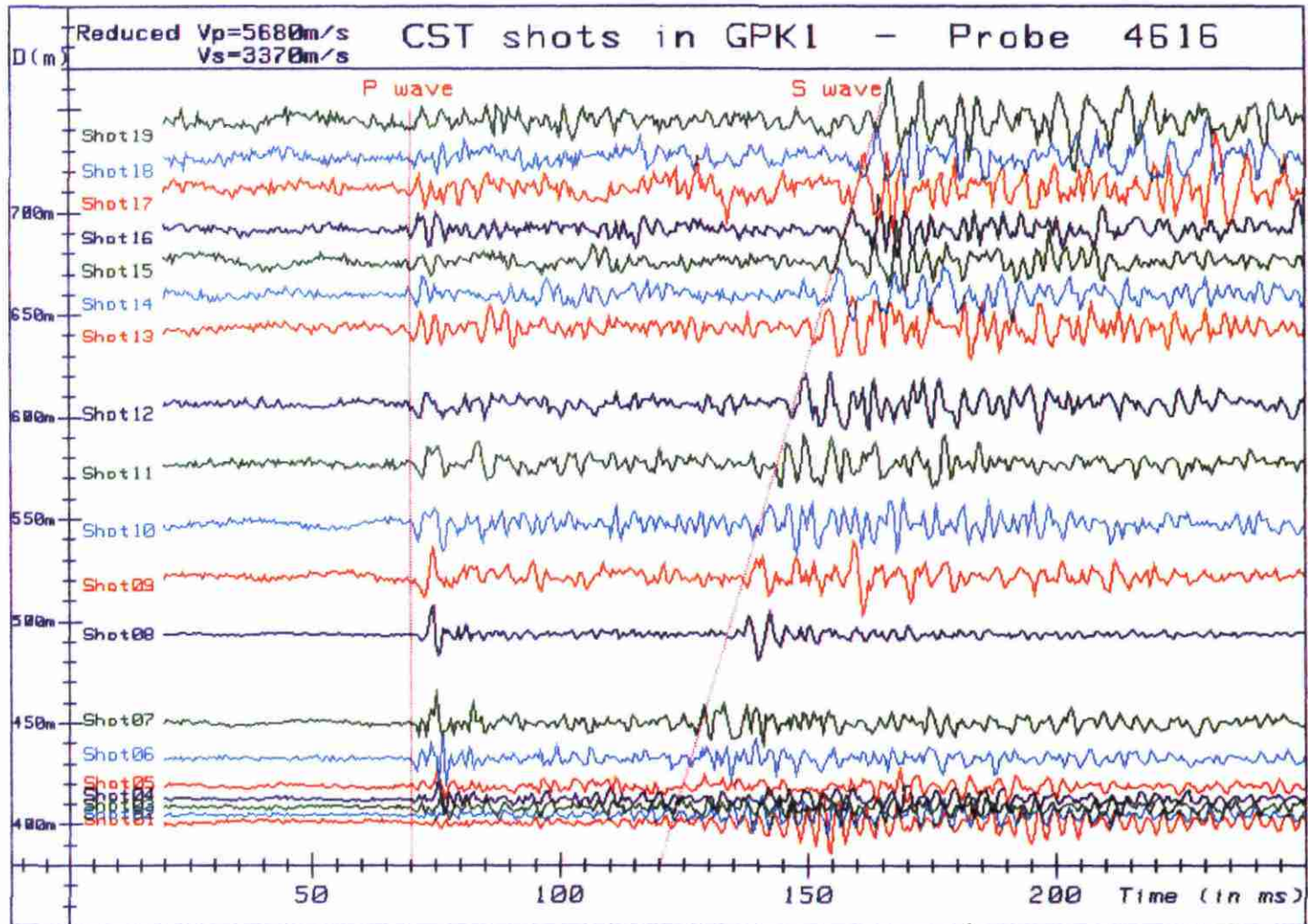


FIGURE 12 - SEISMOGRAMS RECORDED ON PROBE 4616 AS A FUNCTION OF PROPAGATION DISTANCE

the sonic tool around the the borehole. In our case we preferred to use the values given by the second method (i.e. measurement of transit times between GPK1 and 4616), which integrates velocities all along the raypath.

As mentioned above, the quality of the data is worse for the probes sited in the sedimentary cover (i.e. in boreholes 4609 and 4598). However, improvement of this ratio could be obtained on P-wave data,

recorded by shots between 1400 and 1500 m, using cross-correlation and stacking techniques. The idea is to obtain velocity estimates in the Buntsandstein and in the Muschelkalk series where bottom holes of 4609 and 4598 are respectively sited. We could deduce, from the pickings of the P waves on the resulting stacked seismograms, an integrated velocity for the two probes: $V_{p_{4609}} = 4547$ m/s, $V_{p_{4598}} = 4440$ m/s. Knowing the travel distances from the virtual stacked shot to the probe, as well as the velocity inside the granite and the structural model, velocity values inside the Buntsandstein and the Muschelkalk ($V_{p_{bunt.}} = 4330 \pm 30$ m/s; $V_{p_{musc.}} = 3650 \pm 100$ m/s) were derived. Both values fit quite well with the velocity estimates given by the corrected sonic logs (resp. 4410 m/s and 3620 m/s). However, the uncertainty on the deduced P-wave velocity inside the Muschelkalk is very high, due to the small propagation distance inside this series, and to the poor quality of the first arrivals (worse for 4598 than for 4609); in the particular case, of borehole 4598, it was decided to use the velocity value given by sonic logs.

For S waves, the picking of the onsets is too uncertain on probes 4598 and 4609 to obtain accurate V_p/V_s ratio estimates in both series. Hence, it has been decided to use the value obtained in the granite by the CST shots (i.e. 1.689).

In conclusion, the velocity models deduced by the two methods show a velocity difference of only about 1%; the overall geological and velocity model chosen for locating the induced events is given on figure 13.

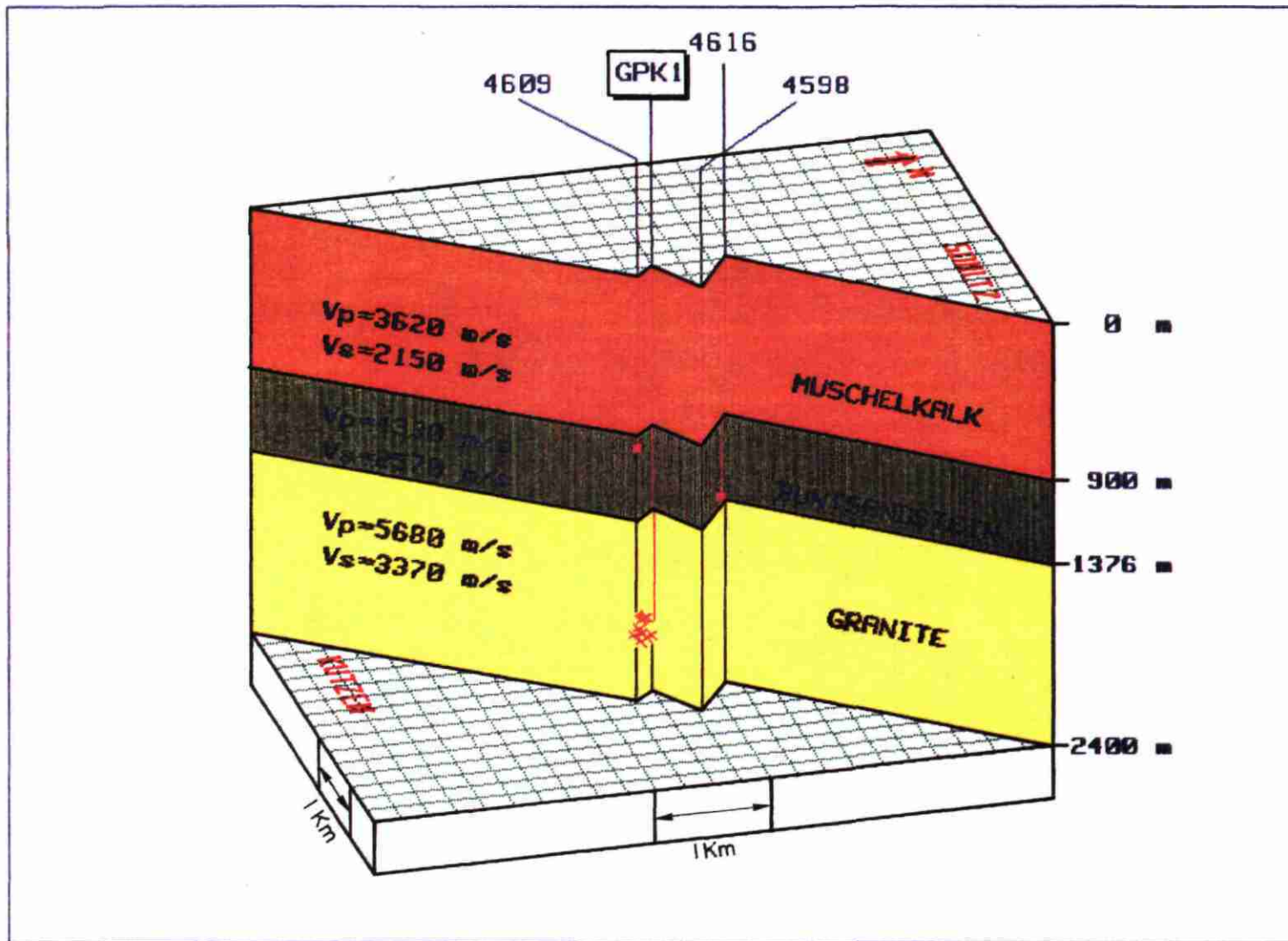


FIGURE 13 - SOULTZ SEISMIC NETWORK. GEOLOGICAL AND VELOCITY MODELS

4. RESULTS OF THE SEISMIC SURVEY DURING STIMULATION IN GPK1

4.1 Description of the hydraulic experiment

A hydraulic stimulation between packers at different levels of the granite in GPK1 was scheduled in an early stage of the project and was to last some weeks. Delays in the progress of the program, and technical problems (due to temperature) with the packers, led to a total duration of the stimulation of only three days. The test was effected over a 30-m-long vertical section of the well, between 1970 m and the bottom.

A total amount of 524 m³ of water was injected between 14 December at 10 a.m. and 16 December at 11 p.m. The water-flow was nearly constant (3.3 l/s), at least during the first 40 hours (Figure 14), except during short periods of several minutes at the beginning. The well-head pressure reached a maximum of 82 bars, corresponding to 47 bars at total depth.

4.2 General results of microseismicity induced during stimulation

Fifty-eight microseisms were induced by the stimulation and no event was recorded during the shut-in period (Beauce A., et al., 1989). Figure 14 shows their rate of occurrence during the survey: the first event occurred only after 2 hours of injection (Figure 15), that is for an injected volume of 25 m³.

Figure 15 illustrates the chronology of the maximum amplitude on channel X of the probe 4616 for the 58 recorded events. The decrease with time of the seismicity (well marked in Figure 14) and of the amplitude (less marked, in Figure 15) can be interpreted as an evolution of the system towards a new stable state.

Figure 16 displays the seismograms for an event with clear wave arrivals on the 3 seismic probes. The difference in amplitude range between signals received on probes 4616 and 4598 reaches about 30 db (500 more meters of sedimentary cover for 4598 than for 4616). A very encouraging result for the method is the occurrence of very sharp P and S waves onsets, which could easily be picked. However, only one fifth of the whole data set (12 out of 58) showed such clear onsets on the three probes.

Results of the spectral analysis carried out on the 58 events using an FFT algorithm on 512 samples (time window of 64 ms) are as follows:

. Resonance (at 200 Hz) of the vertical component of the probe sited in well 4616 is clearly shown, and is likely due to the difficulties encountered while lowering the tool into the borehole, or to a bad anchoring of the probe in the well.

. Power spectra are very similar for all the events, for a given channel of a given probe. This trend is very clear on probe 4616, where most of the onsets are impetus.

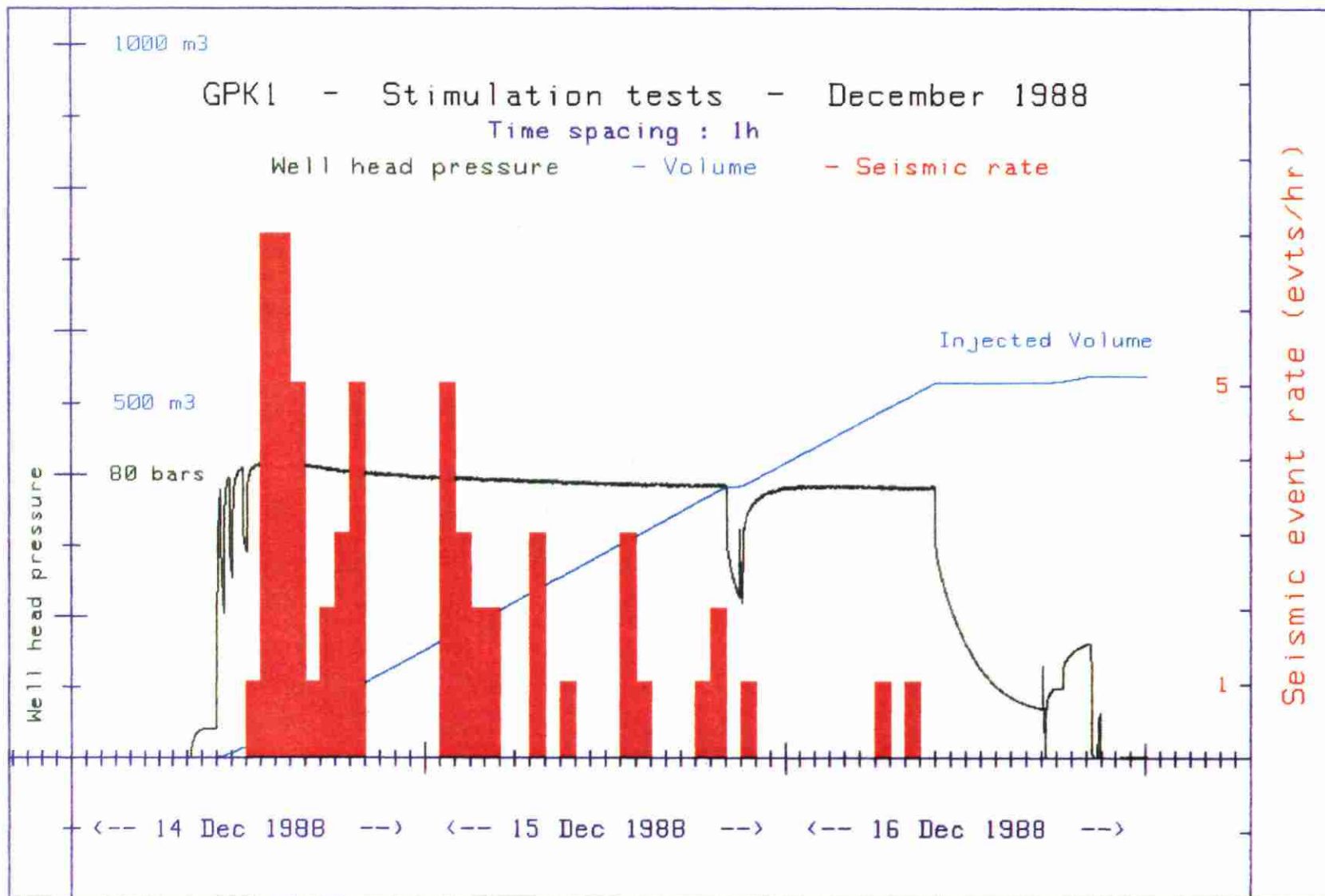


FIGURE 14 - CHRONOLOGICAL DISPLAY OF THE SEISMIC EVENT RATE, INJECTED VOLUME, AND WELL HEAD PRESURE

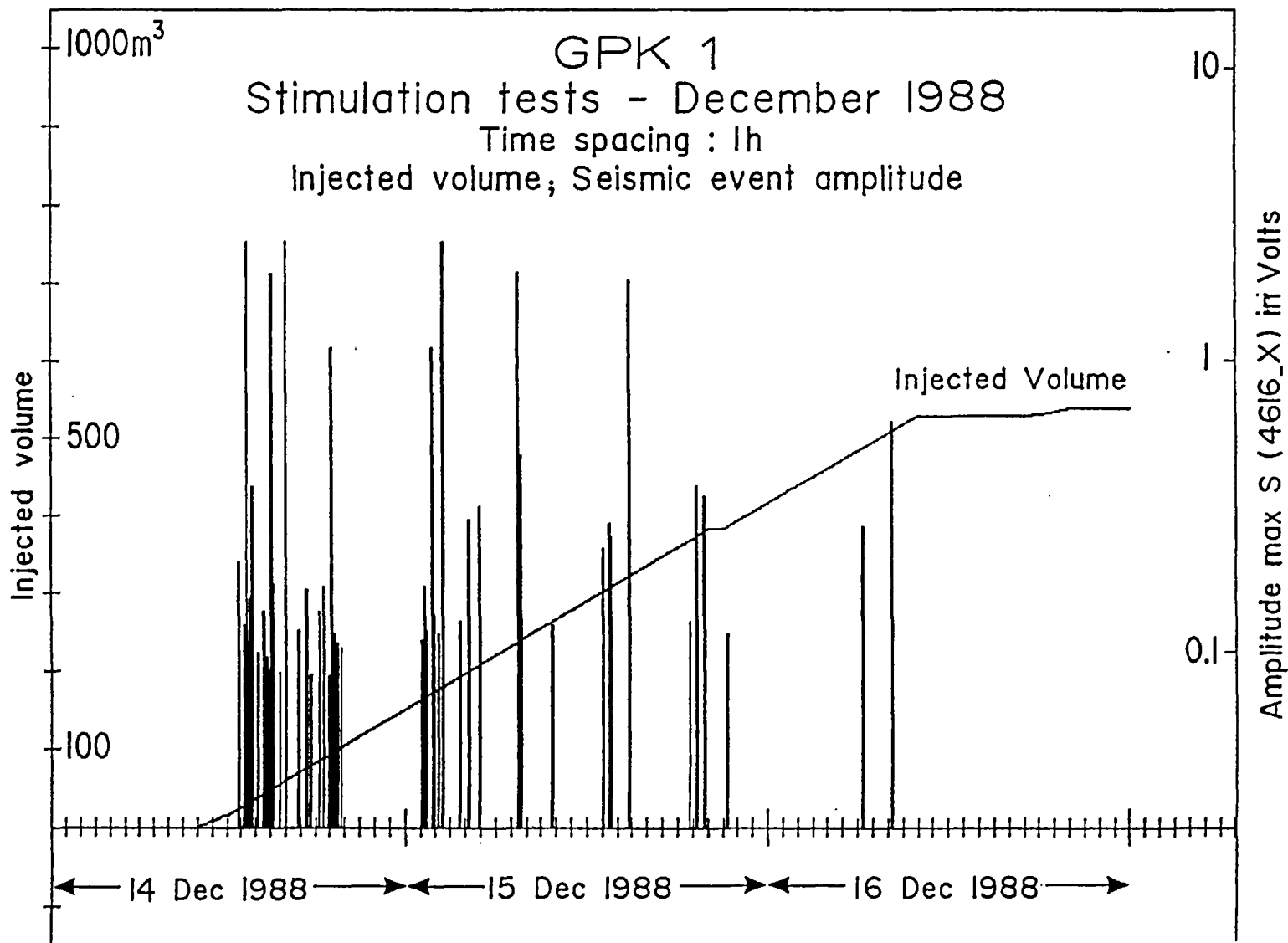


FIGURE 15 - TIME OF OCCURRENCE AND AMPLITUDES OF THE SEISMIC EVENTS RECORDED ON PROBE 4616 DURING STIMULATION

STIMUL05 14 Dec 1988 : 13:19:57

1st POINT: 1

WINDOW : 1000 MILLISEC.

Last POINT: 8000

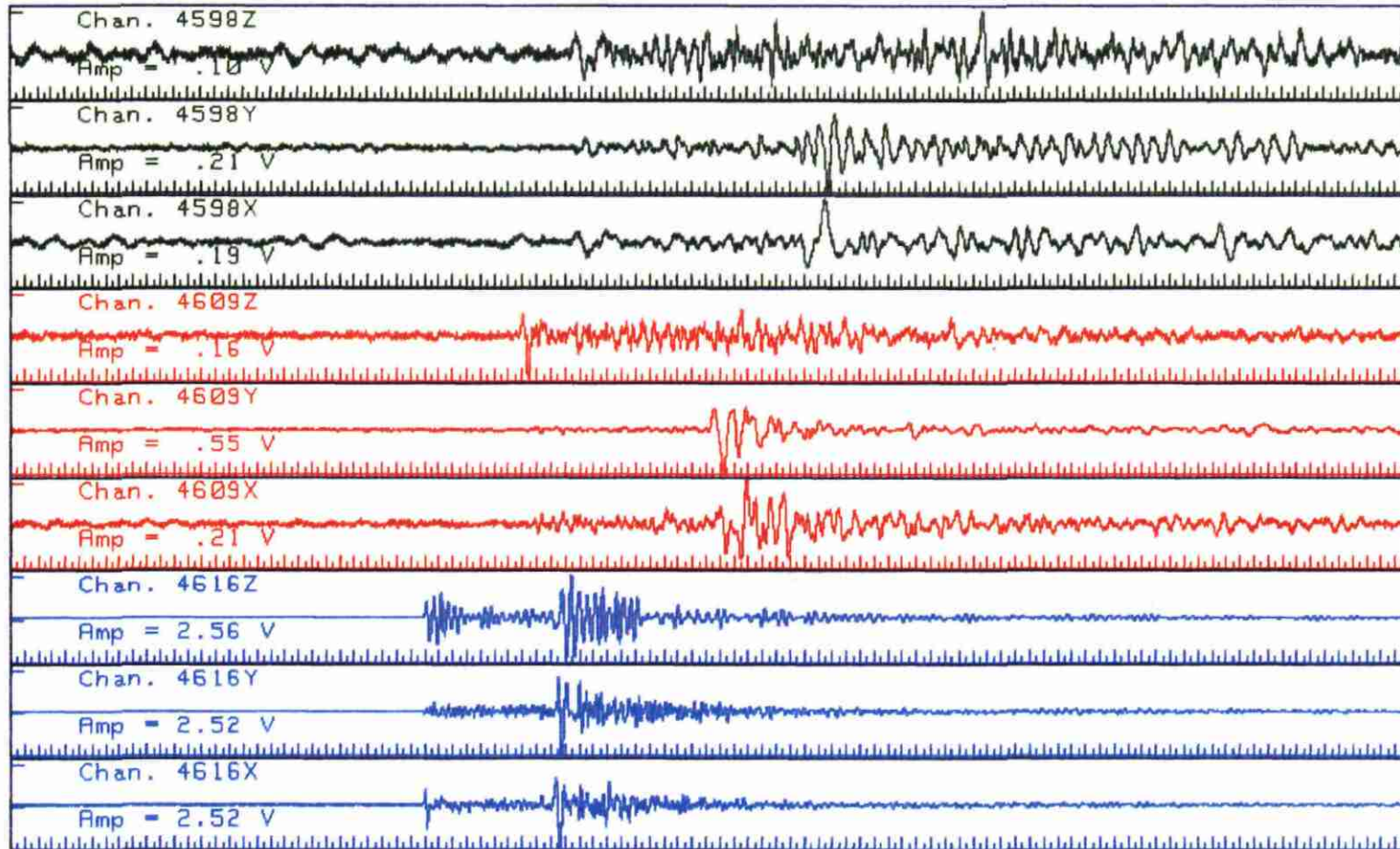


FIGURE 16 - EXAMPLE OF AN INDUCED MICROSEISMIC EVENT

SOULTZ STIMULATION GPK1 12/88 ; Channel X 4616
POWER SPECTRA (db) ; P WAVES ; Nb_fft= 512

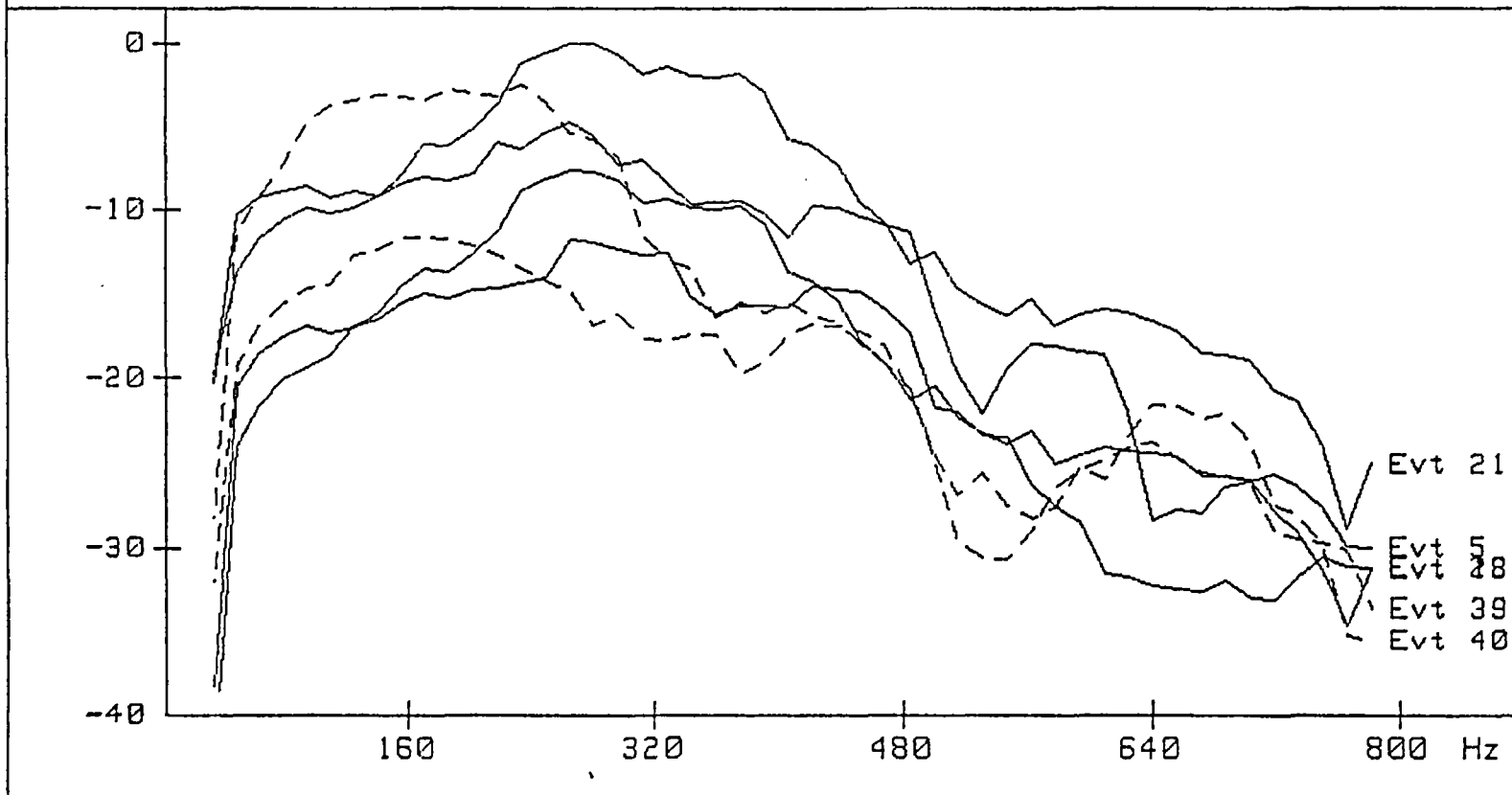


FIGURE 17 - POWER SPECTRA OF SOME CHARACTERISTIC EVENTS

. As expected, the P-wave spectral content is higher (150-300 Hz) for the probe sited in the granite than for the shallower ones (40-200 Hz). Table 3 displays the average frequency of maximum amplitude for the different channels, and the average frequency-band within which the amplitude is not less than 10 dB lower than the maximum.

BOREHOLE	4616		4609		4598	
CHANNEL	X	Z	Y	Z	Y	Z
Fmax P (Hz)	300±20	200±10	125	160	110	120
Fp - band (Hz) down to -10 dB	100-480	150-280	40-250	40-250	40-200	40-200
Fmax S (Hz)	250±20	200	100	150	100	100
Fs - band (Hz) down to -10 dB	100-400	120-300	30-150	30-230	20-160	30-200

Table 3: Spectral analysis of the hydraulically induced seismic events. General trends.

A slight exception to these general trends occurs for events 39 and 40, which present a lower spectral content (170 Hz for the X-4616 component instead of the 300 Hz generally observed - Figure 17).

Except for these two events, all the others display similar characters and spectral contents, which suggests repeated movements along the same joints or fractures.

Figure 18 shows the bi-modal distribution of the differences (Ts-Tp) between S and P arrival times on probe 4616 for the 58 events: 13 events with (Ts-Tp) between 91 and 95 ms, and 39 ones between 99 and 109 ms. This corresponds to at least two focal zones. (Ts-Tp) differences observed on the events recorded on probe 4616, versus time, are plotted in figure 19. Although seismic activity starts and continues simultaneously for the two families, the seismic-energy-release patterns are rather different. For the group closest to 4616, the events of higher magnitudes occur at the beginning of the microseismic emission, whereas for the other group, the higher magnitudes are observed after 16 h of pumping, which can be due to propagation delay of the pressure. This trend supports the assumption of the existence of two families that are not linked to the same fracture. But, even if they are distinct, they were affected by the same mechanism, since their signatures for a given probe are similar.

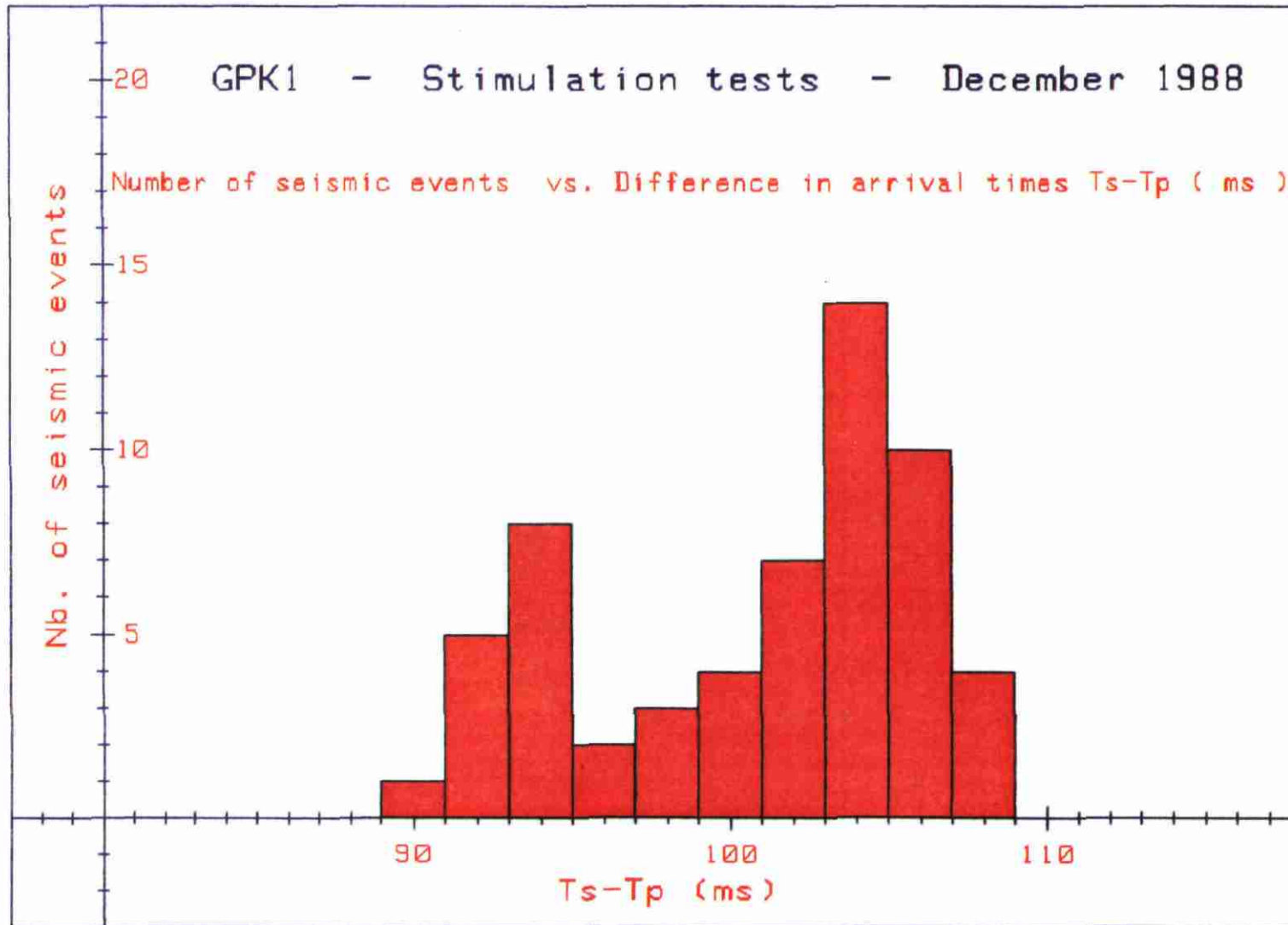


FIGURE 18 - NUMBER OF SEISMIC EVENTS VS. DIFFERENCE IN ARRIVAL TIMES ($T_s - T_p$) ON PROBE 4616

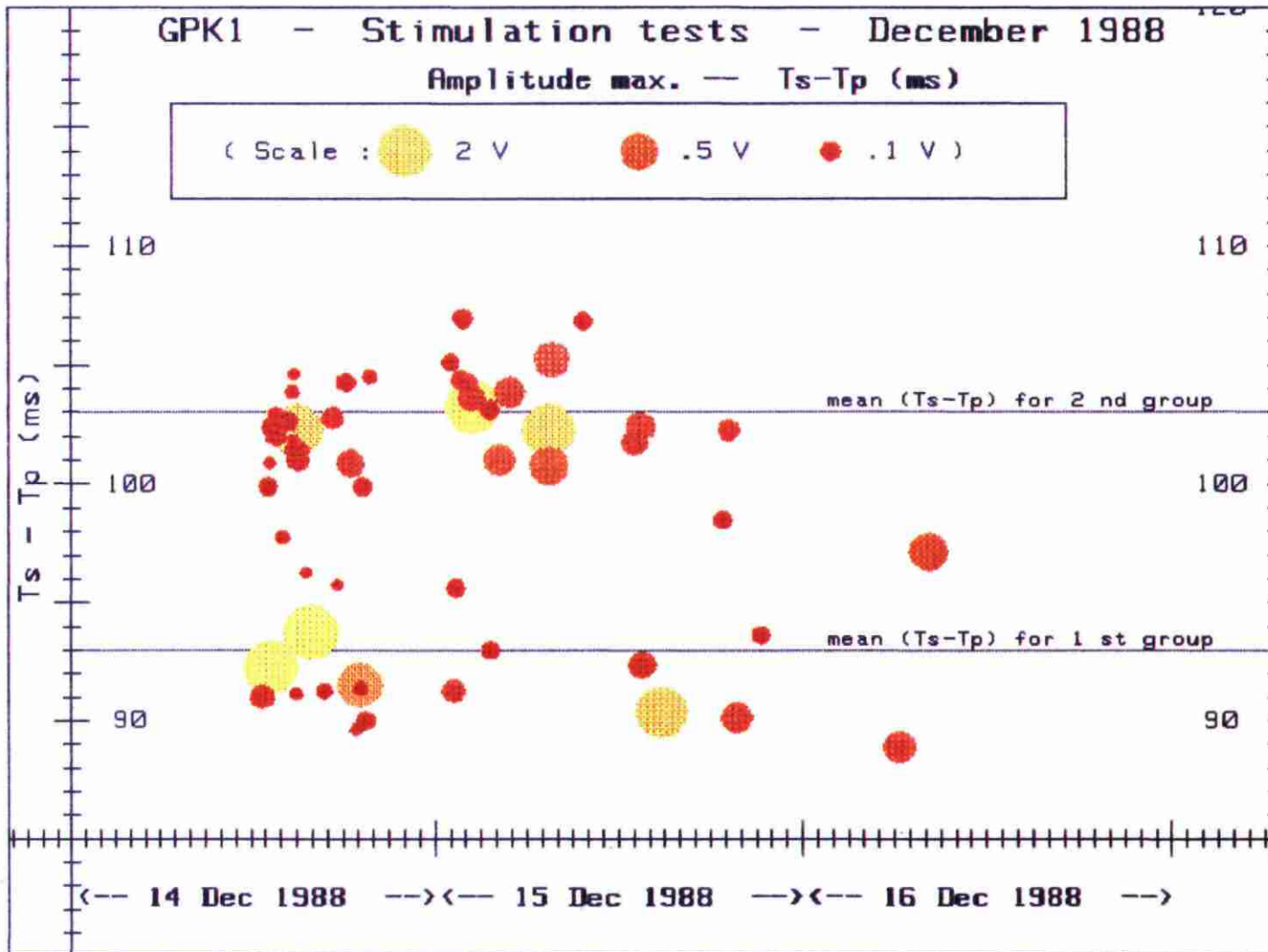


FIGURE 19 - S AND P ARRIVAL TIME DIFFERENCES AS A FUNCTION OF TIME AND DISTRIBUTION OF THE MAXIMUM AMPLITUDES RECORDED ON PROBE 4616

4.3 Location of the events

Only 12 events out of the whole data set were selected, as the other ones did not allow an accurate enough P- or S- wave picking on the seismograms recorded by the probes sited in the sedimentary cover. These 12 events are nearly uniformly spaced in time throughout the experiment and, consequently, are representative of the whole recorded seismicity.

Using both P- and S-wave arrival times observed on the sensors sited in borehole 4616, and the model presented in figure 13, we calculated the origin time of the events. A 3-D grid (mesh size 20 m) of points surrounding GPK1's bottom was defined and, taking into account ray refractions at the different interfaces, theoretical P and S- wave propagation times from the nodes of this grid to each of the 3 probes were calculated. Intersections of the surfaces representing the possible source locations compatible with the observed propagation times on each probe for both P and S waves, define a narrow zone from where the event originates.

Figure 20 illustrates the location method used. Each square represents the grid set for a constant longitude (X -constant); vertical axis stands for depth, and horizontal axis for latitude. Inside each square, the possible source locations obtained for both P and S waves are represented by curves named (P1,S1), (P2,S2) and (P3,S3) for probes in boreholes 4616, 4609 and 4598, respectively. We can note that curves (P1,S1) coincide since the origin time is calculated using the data of probe 4616. Now, as a function of changing longitude, one can observe focusing and defocusing of the locus intersections obtained for P waves (resp. S waves). Intersections of the curves P1, P2, P3 (resp. S1, S2, S3) are then considered as two possible source locations. Final hypocenter coordinates are chosen as the center of these two estimates. The dispersion observed for the whole data set is around 10 m.

Figure 21 displays the projections of the 12 calculated hypocenters on three orthogonal planes (map view and E-W,N-S vertical cross-sections passing by GPK1). Two interpretations can be given following the way the hypocenters are associated.

The first one (Figure 21-1) groups the events according to their depth distribution. Two active zones can be distinguished: the first one associates the events clustered close to GPK1 borehole wall, and the second one gathers the 7 other events, more widely spread out on a sub-horizontal plane at 2090 m depth. In this case, the second active zone may be related to a reflector (event 5 in Figure 8) observed on the WSP section and on the re-processed 84 J seismic reflection profile.

The second interpretation groups together 9 events (Figure 21-2) along a sub-vertical plane orientated N160-170°. This interpretation, although disregarding 3 microseisms (very close in time) whose origin cannot be deduced with the available data, is in better accordance with the fault F2 observed on the WSP which may connect the active zones at 2000 and 2100 m depth. This last interpretation seems to be satisfactory with respect to the maximal horizontal-stress component deduced by BHTV data analysis (N170°) and by in-situ stress measurements (N145°). Moreover, the fact that all the recorded events present similar signatures for a given probe, is in better accordance with this interpretation.

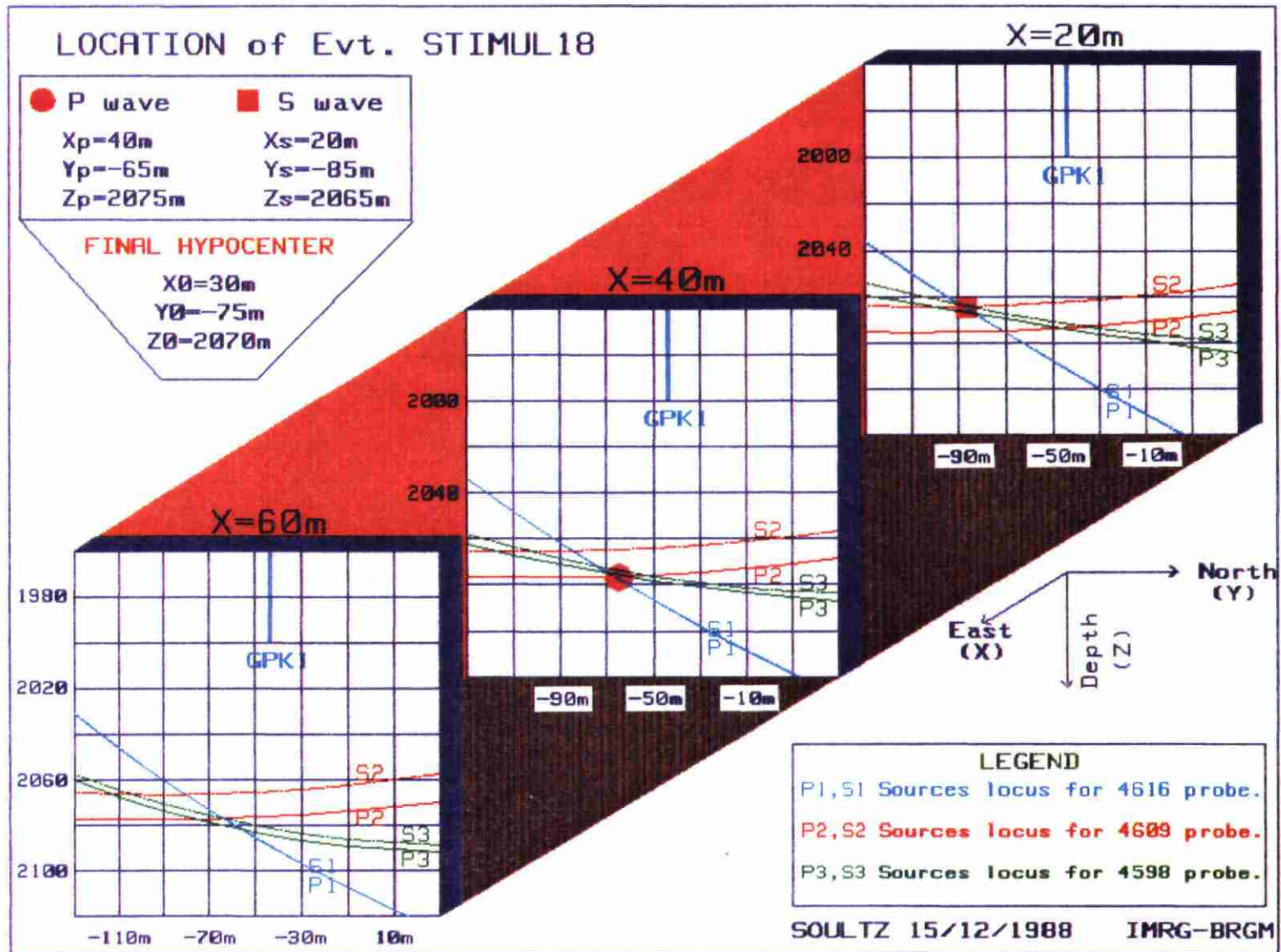


FIGURE 20 - EXAMPLE OF LOCATION PROCESSING FOR EVENT N° 18

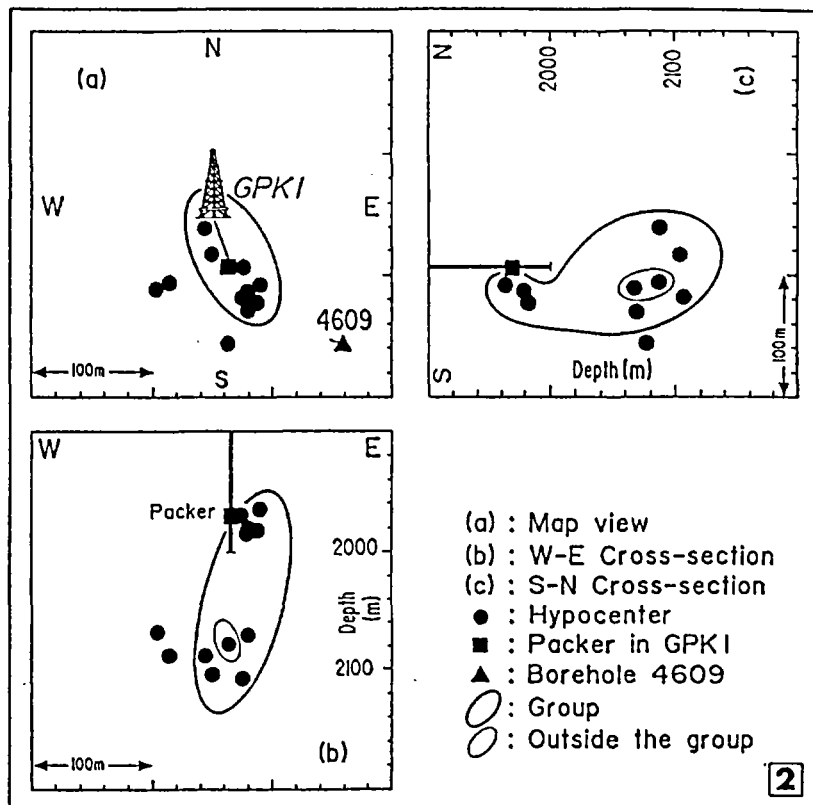
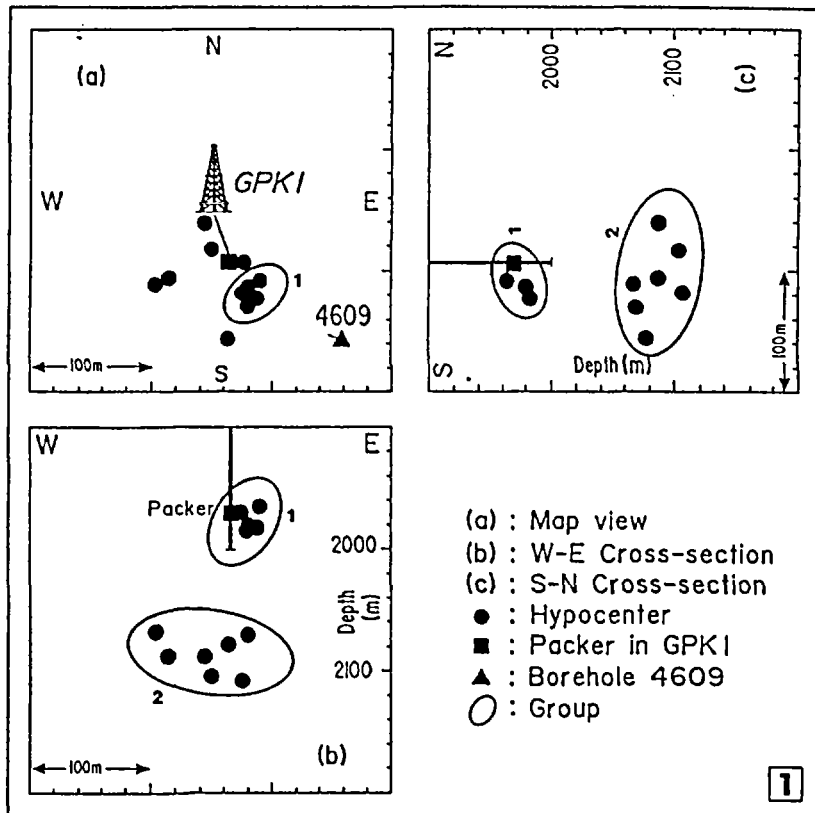


FIGURE 21 - MICROSEISMIC EVENTS DISTRIBUTION AND INTERPRETATIONS

- 1** Subhorizontal planes
- 2** Subvertical plane

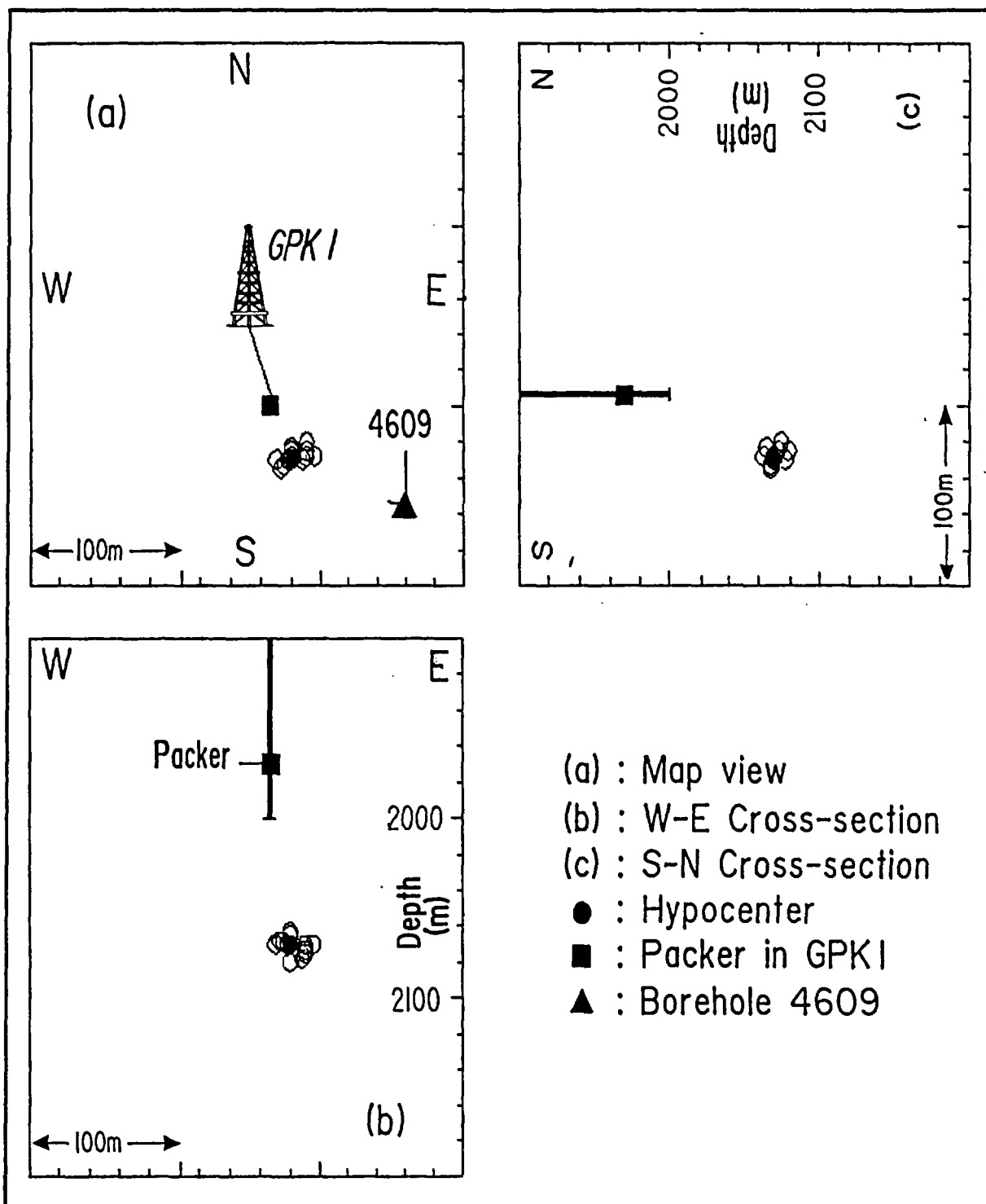


FIGURE 22 - HYPOCENTERS OBTAINED FOR A ± 1 MS DISTURBANCE IN THE ARRIVAL TIMES (EVENT 18)

In any case, the lack of data does not allow to go really further on these assumptions.

To estimate the precision of the resulting locations, observed arrival times were artificially disturbed by ± 1 ms, successively on the different probes. Illustration of the obtained locations for event 18 for 12 attempts is presented in figure 22, which shows a ± 15 m shift around the initial location. The influence of different Vp/Vs ratios (1.66 and 1.73), for the sedimentary layers only, was also modelled, leading to a spatial uncertainty of ± 15 m in the final locations.

The combined location error is of the order of ± 30 m.

5. CONCLUSIONS

Despite a rather low flow-rate (3.3 l/s) and a low bottom-hole pressure (47 bars), a notable seismicity was recorded during the stimulation experiment undertaken at Soultz in December 1988. This seismicity decreased with time (event-rate and magnitudes), indicating that the system had reached a new steady state. This result has been made possible by the proper design of specific, permanently-installed, geophones suited to the rough downhole temperature and corrosion conditions.

Location results indicate that two zones of weakness were concerned during the experiment: a first one close to the top of the injection zone in GPK1 borehole, and another one 100 m deeper than the bottom of the hole. The propagation direction of the seismicity from the borehole is consistent with the maximum horizontal-stress orientation. Signatures of the events are similar for the whole data set, suggesting that the involved rupture mechanism has been the same all over the stimulation experiment.

According to a first interpretation, the second active group can be related to a seismic horizon pointed out by the VSP survey and the re-processing of the existing seismic reflection profile. In a second interpretation, the two active zones might be connected through a N160-170° sub-vertical feature observed during the WSP experiment. However, it is obvious that more data are needed to confirm or to invalidate these assumptions and the general trends pointed out.

To locate the events, the hodogrammetry method has failed: accurate results were not obtained, mainly because of the too low precision in the orientations of the probes from surface shots (complex tectonic context of the Soultz site).

The active seismic survey shows marked reflectors inside the granite at 1590, 1640 and 1820 m depth, that can be easily correlated with altered zones known from borehole logging. Two major fractures are observed on the WSP between 1650 and 2200 m, one dipping NE, and the other one dipping SW, both being sited at some tens of meters from GPK1. Moreover, two more reflectors are found beneath the bottom of the well, at about 2000 and 2100 m depth. All these results are compatible with the locations of the two active zones of induced seismic events.

The reprocessing of the seismic-reflection sections indicates, at this stage of the interpretation, that one or two coherent events exist near GPK1, that could be linked to the reflectors mentioned above.

The feasibility of such a seismic array to monitor artificially created or re-opened fractures is confirmed by the present work, but the results also pointed out the necessity of more than three observation boreholes. To obtain more reliable results and to be able to use all the data recorded on the network, these probes must be furthermore sited inside the granite where attenuation effects are less dramatic. This will be undertaken within the second phase of the project.

REFERENCES

- BARIA R., GREEN A.S.P. (1989) - Microseismics: a key to understanding reservoir growth. International HDR Conference, Camborne (UK), 27-30 June 1989.
- BEAUCE A., COURTOT P., FABRIOL H., LE MASNE D. (1988) - Surveillance sismique sur le champ pétrolier de Villeperdue (Marne). BRGM Reports n° 88 EEE/IRG 022 and 028.
- BEAUCE A., FABRIOL H., LE MASNE D., CAVOIT C., MECHLER P., CHEN X. (1989) Seismic monitoring on the Soultz site. International HDR Conference, Camborne (UK), 27-30 June 1989.
- BEAUCE A., FABRIOL H., LE MASNE D. (1989) - Seismicity induced during a hydraulic stimulation at the Soultz-sous-Forêts HDR Geothermal Project. 59th Annual International SEG meeting, Dallas, Nov. 1989, Vol I, 241-243.
- CAUTRU J.P. (1989) - Coupe géologique passant par le forage GPK1 calée sur la sismique reflexion. IMRG Document.
- CAVOIT C. (1989) - Etude, réalisation et mise en oeuvre d'un système de trois sondes sismiques de fond de forage. CNRS (Report CRG 20 JAN 89).
- CORNET F.H. (1988) - Geothermie Profonde Généralisée. Projet Mayet de Montagne. Etude in situ de la percolation forcée d'eau en milieu granitique. GPG final report September 1988.
- GENTER A. (1989) - Geothermie Roches Chaudes Sèches. Le granite de Soultz-sous-Forêts. Fracturation naturelle, altérations hydrothermales et interactions eau-roche. Orléans University Thesis - 30 October 1989.
- KAPPELMEYER O., GERARD A. (1989) - The European geothermal project at Soultz-sous-Forêts. Proceedings of the 4th International Seminar on the results of E.C. Geothermal energy research and demonstration. Florence 27-30 April 1989. pp. 283-334.
- MOCK J. (1989) - The U.S. Hot Dry Rock programme. International Hot Dry Rock Geothermal Energy Conference, Camborne (U.K.), 27-30 June 1989.
- PARKER R.H. (1989) - The background to Phase 3 of the Camborne School of Mines Geothermal Energy Project. International Hot Dry Rock Geothermal Energy Conference, Camborne (U.K.), 27-30 June 1989.
- RUMMEL F., HANSEN J. - Stress measurements in HDR research, RCS Workshop, Strasbourg, 6-7 December 1988, 1 p.

